
Keep It on a Leash: Controllable Pseudo-label Generation Towards Realistic Long-Tailed Semi-Supervised Learning

Yixin Hou¹, Bo Han¹, Yuheng Jia^{1,2,3*}, Hui Liu³, Junhui Hou⁴

¹School of Computer Science and Engineering, Southeast University, Nanjing 210096, China

²Key Laboratory of New Generation Artificial Intelligence Technology and Its Interdisciplinary Applications (Southeast University), Ministry of Education, China

³School of Computing Information Sciences, Saint Francis University, Hong Kong, China

⁴Department of Computer Science, City University of Hong Kong, Hong Kong, China

yixin@seu.edu.cn, hanbo@seu.edu.cn, yhjia@seu.edu.cn,
h2liu@sfu.edu.hk, jh.hou@cityu.edu.hk

Abstract

Current long-tailed semi-supervised learning methods assume that labeled data exhibit a long-tailed distribution, and unlabeled data adhere to a typical predefined distribution (i.e., long-tailed, uniform, or inverse long-tailed). However, the distribution of the unlabeled data is generally unknown and may follow an arbitrary distribution. To tackle this challenge, we propose a Controllable Pseudo-label Generation (CPG) framework, expanding the labeled dataset with the progressively identified reliable pseudo-labels from the unlabeled dataset and training the model on the updated labeled dataset with a known distribution, making it unaffected by the unlabeled data distribution. Specifically, CPG operates through a controllable self-reinforcing optimization cycle: (i) at each training step, our dynamic controllable filtering mechanism selectively incorporates reliable pseudo-labels from the unlabeled dataset into the labeled dataset, ensuring that the updated labeled dataset follows a known distribution; (ii) we then construct a Bayes-optimal classifier using logit adjustment based on the updated labeled data distribution; (iii) this improved classifier subsequently helps identify more reliable pseudo-labels in the next training step. We further theoretically prove that this optimization cycle can significantly reduce the generalization error under some conditions. Additionally, we propose a class-aware adaptive augmentation module to further improve the representation of minority classes, and an auxiliary branch to maximize data utilization by leveraging all labeled and unlabeled samples. Comprehensive evaluations on various commonly used benchmark datasets show that CPG achieves consistent improvements, surpassing state-of-the-art methods by up to **15.97%** in accuracy. The code is available at <https://github.com/yaxinhou/CPG>.

1 Introduction

Over the past decade, semi-supervised learning (SSL) has emerged as a mainstream paradigm for enhancing the performance of deep neural networks (DNNs) in label-scarce domains like medical diagnosis [1, 2, 3] by leveraging abundant unlabeled data. The dominant SSL framework utilizes unlabeled samples by generating pseudo-labels from high-confidence model predictions [4, 5, 6]. However, conventional SSL methods [7, 8, 9] rely on the unrealistic assumption of balanced and aligned distributions for labeled and unlabeled data. Long-tailed semi-supervised learning (LTSSL) [10, 11, 12]

*Corresponding author.

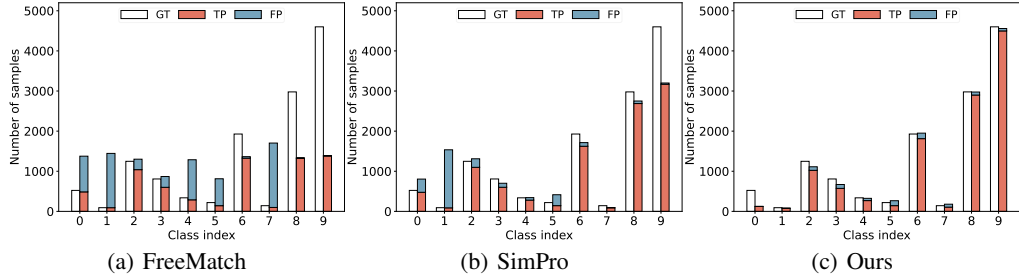


Figure 1: Comparison of pseudo-label predictions among FreeMatch [8], SimPro [13], and our CPG under arbitrary unlabeled data distribution. GT denotes the ground-truth unlabeled data distribution. TP (FP) denotes the predicted true (false) positive pseudo-labels. The dataset is CIFAR-10-LT with $(N_{max}, M_{max}, \gamma_l, \gamma_u) = (400, 4600, 50, 50)$, where N_{max} (M_{max}) denotes the number of samples in the most frequent class of the labeled (unlabeled) dataset, while γ_l (γ_u) denotes the imbalance ratio of the labeled (unlabeled) dataset. Our CPG can generate more reliable pseudo-labels than FreeMatch and SimPro in both minority classes like class 1, 2, and majority classes like class 8, 9.

relaxes the balance assumption, however, it still suffers from potential distribution mismatches between labeled and unlabeled data.

A motivating example. In urban traffic monitoring systems, vehicle images captured by surveillance cameras are classified into distinct categories (e.g., bicycles, trucks, motorcycles) based on their visual characteristics. This presents a long-tailed semi-supervised learning scenario, where labeled data exhibit a long-tailed distribution (with common vehicles like cars dominating and specialized vehicles like ambulances being underrepresented). Meanwhile, unlabeled data collected across different urban environments share the same vehicle categories but may exhibit unknown distributional shifts. These distributional shifts arise from spatial variations (e.g., higher proportions of personal vehicles in residential areas) or temporal fluctuations (e.g., increased taxi frequency during rush hours).

Recent advances in realistic long-tailed semi-supervised learning (ReALTSSL) have attempted to address the distribution mismatch between labeled and unlabeled data. For instance, ACR [14] adjusts logits based on the distance between the estimated unlabeled data distribution and the predefined anchor distributions, while CPE [15] employs multiple classifiers (experts) to model diverse unlabeled data distributions. Although effective, both methods assume that unlabeled data adhere to a typical predefined distribution (i.e., long-tailed, uniform, or inverse long-tailed), which may not hold in practice. The recent method SimPro [13] alleviates this limitation through an Expectation-Maximization (EM)-based pseudo-labeling method. However, as illustrated in Fig. 1(b), SimPro’s distribution estimation ability degrades when unlabeled data follow an unknown arbitrary distribution. In summary, existing methods rely on a confidence threshold to select high-confidence pseudo-labels for distribution estimation, which subsequently guides pseudo-label generation. However, as shown in Figs. 1 and 3, this strategy becomes unreliable when handling the unknown arbitrary unlabeled data distribution, as high-confidence pseudo-labels may still contain substantial errors. These inaccuracies propagate during training, resulting in confirmation bias and model performance degradation.

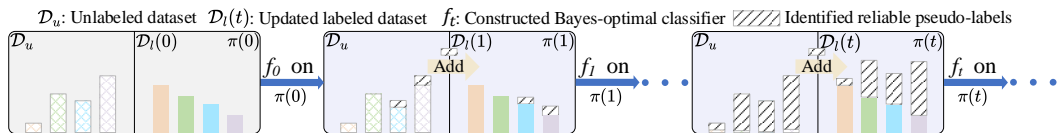


Figure 2: Overview of the controllable self-reinforcing optimization cycle.

To address these challenges, we introduce a Controllable Pseudo-label Generation (CPG) framework that employs a controllable self-reinforcing optimization cycle to handle the unknown arbitrary unlabeled data distribution problem in ReALTSSL. As illustrated in Fig. 2, CPG utilizes a dynamic controllable filtering mechanism to identify reliable pseudo-labels. These reliable pseudo-labels are combined with the labeled dataset to construct an updated labeled dataset $D_l(t)$ with a known distribution $\pi(t)$. We then construct a Bayes-optimal classifier f_t via logit adjustment [16] based on the known distribution $\pi(t)$. Note that the Bayes-optimal classifier is unaffected by the unlabeled data distribution. The Bayes-optimal classifier f_t , in turn, helps identify more reliable pseudo-labels in the next training step. Through this optimization cycle, an increasing number of unlabeled samples are progressively incorporated as reliable ones, enabling the framework to capture the unlabeled data distribution in later training stages implicitly (See Fig. 5 in Appendix A). Theoretically, we prove

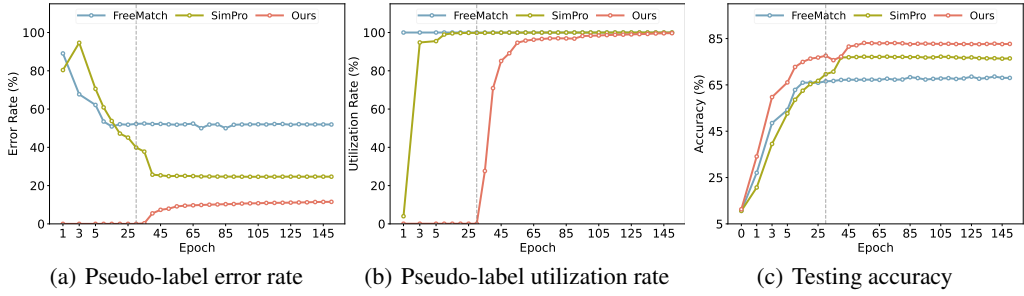


Figure 3: Comparison of pseudo-label error rate (a), pseudo-label utilization rate (b), and testing accuracy (c) among FreeMatch [8], SimPro [13], and our CPG under arbitrary unlabeled data distribution. The dataset is CIFAR-10-LT with $(N_{max}, M_{max}, \gamma_l, \gamma_u) = (400, 4600, 50, 50)$. The vertical gray dotted line indicates the initiation of pseudo-labeling in our method. Our CPG can generate pseudo-labels with a lower error rate and comparable utilization rate, achieving superior testing accuracy compared to both FreeMatch and SimPro.

that this optimization cycle can significantly reduce the generalization error under some conditions. Empirically, Fig. 1(c) shows the superior pseudo-label prediction ability of our method.

To further improve our CPG, we introduce a class-aware adaptive augmentation (CAA) module and an auxiliary branch. The CAA module enhances minority class representations by dynamically adjusting augmentation intensity based on class compactness. Specifically, for classes with higher compactness (indicating lower intra-class diversity), CAA applies a smaller augmentation radius during representation synthesis to refine decision boundaries more effectively. Meanwhile, the auxiliary branch maximizes data utilization by enforcing prediction consistency between different augmentation views of all labeled and unlabeled samples.

In summary, the main contributions of this work are as follows.

- We propose a Controllable Pseudo-label Generation (CPG) framework to handle the unknown arbitrary unlabeled data distribution problem in ReaLTSSL. The framework expands the labeled dataset with the progressively identified reliable pseudo-labels from the unlabeled dataset, and trains the model on the updated labeled dataset with a known distribution, making it unaffected by the unlabeled data distribution.
- We theoretically prove that our controllable self-reinforcing optimization cycle can significantly reduce the generalization error under some conditions.
- We further propose a class-aware adaptive augmentation module to enhance the representation of minority classes, and an auxiliary branch to maximize data utilization by leveraging all labeled and unlabeled samples.
- Comprehensive experiments on four commonly used benchmarks (CIFAR-10-LT, CIFAR-100-LT, Food-101-LT, and SVHN-LT) under various labeled and unlabeled data distributions validate that our CPG achieves new state-of-the-art performances with a **15.97%** maximum improvement.

2 Related Work

Long-Tailed Learning (LTL) addresses the challenge of training effective models on data with long-tailed distributions, where a majority of classes are represented by only a few samples. Prevailing LTL methods can be categorized into three groups: re-sampling, logit adjustment, and ensemble learning. Re-sampling [17, 18, 19, 20] balances classes by under-sampling majority classes or over-sampling minority classes. Logit adjustment [21, 22, 23] modifies the predicted logits to compensate for class imbalance. Ensemble learning [24, 25, 26] combines multiple classifiers (experts) to improve the performance and robustness of the model. Despite their success in supervised learning, extending them to long-tailed semi-supervised learning (LTSSL) requires extra effort, as exploiting unlabeled samples is not trivial.

Semi-Supervised Learning (SSL) provides a powerful framework for improving model performance in label-scarce domains by leveraging abundant unlabeled data. Early SSL methods rely on self-training with pseudo-labeling, where model refinement depends on the quality of generated pseudo-

labels. Recent advances integrate pseudo-labeling [5, 6] with consistency regularization [27, 28], enforcing prediction invariance between weak and strong augmentation views to enhance robustness. Prominent examples include FixMatch [7], FlexMatch [29], FreeMatch [8], SoftMatch [9], and SemiReward [30], which primarily differ in their confidence thresholding strategies to balance pseudo-label quality and quantity. While effective in settings with balanced labeled and unlabeled data distributions, these methods struggle with long-tailed labeled data or mismatched distributions between labeled and unlabeled data.

Long-Tailed Semi-Supervised Learning (LTSSL) addresses the challenges arising from the long-tailed distribution. Existing LTSSL methods integrate long-tailed learning techniques [31, 32, 33, 34, 35] with frameworks like FixMatch. For example, ABC [10] employs an auxiliary classifier to improve minority class generalization, CReST [36] selectively generates pseudo-labels for minority class samples based on class frequency, and CoSSL [11] introduces feature enhancement strategies to refine classifier learning. However, these approaches overlook distribution mismatches between labeled and unlabeled data, a key limitation addressed by realistic long-tailed semi-supervised learning (ReaLTSSL). Recent ReaLTSSL methods include ACR [14], which adjusts logits based on the distance between the estimated unlabeled data distribution and the predefined anchor distributions; CPE [15], which employs multiple classifiers (experts) to model diverse unlabeled data distributions; Meta-Expert [37], which significantly enhances CPE by incorporating the expertises of different experts, and SimPro [13], which estimates unlabeled data distributions through high-confidence pseudo-label counts and adapts pseudo-label generation probabilities correspondingly. *Despite their contributions, ACR, CPE, and Meta-Expert require prior knowledge of the unlabeled data distribution. SimPro, meanwhile, fails to estimate the unlabeled data distribution accurately when the labeled and unlabeled distributions diverge significantly. These limitations restrict their practical applicability.*

3 Proposed Method

3.1 Preliminaries

Problem formulation and challenges. In ReaLTSSL, we consider a labeled dataset $\mathcal{D}_l = \{x_i^l, y_i^l\}_{i=1}^N$ of size N and an unlabeled dataset $\mathcal{D}_u = \{x_j^u\}_{j=1}^M$ of size M , where both datasets share identical feature and label spaces. Here, x_i^l denotes the i -th labeled sample with ground-truth label $y_i^l \in \{1, \dots, C\}$, x_j^u represents the j -th unlabeled sample, and C is the total number of classes. Let N_c denote the number of labeled samples in class c , defining the labeled data imbalance ratio as $\gamma_l = \frac{\max_c N_c}{\min_c N_c}$. While we can theoretically assume that M_c represents the number of samples for class c in \mathcal{D}_u , with its imbalance ratio $\gamma_u = \frac{\max_c M_c}{\min_c M_c}$, in practice the unlabeled data follow an unknown arbitrary distribution, making M_c and γ_u unavailable. The goal of ReaLTSSL is to train a classifier $F : \mathbb{R}^d \rightarrow [1, \dots, C]$, parameterized by θ , using \mathcal{D}_l and \mathcal{D}_u to achieve robust generalization across all classes. This presents a key challenge for SSL and LTSSL methods, as most existing methods depend on either balanced or aligned distributions between \mathcal{D}_l and \mathcal{D}_u , or require prior knowledge of the unlabeled data distribution. In practice, the distribution of \mathcal{D}_u is typically unknown, limiting the capability of the existing methods.

Logit adjustment. In real-world scenarios, data typically follow a long-tailed distribution, resulting in models trained on such data exhibiting an inherent bias toward majority classes. To mitigate this issue, numerous long-tailed learning methods aim to enhance minority class performance without degrading accuracy in majority classes. A prominent approach, logit adjustment [16], promotes larger relative margins between the minority positive and majority negative classes. It has been theoretically established as the Bayes-optimal solution for long-tailed learning. The logit-adjusted softmax cross-entropy loss (LA loss, ℓ_{la}) is defined as:

$$\ell_{la}(y, f(g(x))) = -\log \frac{e^{f_y(g(x)) + \ln P_y}}{\sum_{y' \in [C]} e^{f_{y'}(g(x)) + \ln P_{y'}}}, \quad (1)$$

where $g(\cdot)$ and $f(\cdot)$ denote the encoder and classifier, respectively, $f_y(g(x))$ is the predicted logit of the y -th class, and P_y denotes the class prior of the y -th class.

3.2 Our CPG Framework

Framework overview. To address the above-mentioned challenges, we introduce CPG, a controllable pseudo-label generation framework tailored for ReaLTSSL that operates *without* restrictive assumptions or prior knowledge about the distribution of the unlabeled dataset. Specifically, CPG adopts a controllable self-reinforcing optimization cycle, a class-aware adaptive augmentation module, and an auxiliary branch. The first employs a dynamic controllable filtering mechanism to identify reliable pseudo-labels. These pseudo-labels are combined with the original labeled dataset to iteratively update the labeled dataset, and progressively construct a Bayes-optimal classifier through logit adjustment. The improved classifier, in turn, helps identify more reliable pseudo-labels for subsequent training steps. The second enhances discriminative representations for minority classes within each training step. The last maximizes data utilization by leveraging all labeled and unlabeled samples. *Unlike existing methods that estimate the unlabeled data distribution based on high-confidence pseudo-labels, our CPG incorporates reliable pseudo-labels from the unlabeled dataset into the labeled dataset, and trains the model on the updated labeled dataset with a known distribution, making it unaffected by the unlabeled data distribution.*

Controllable self-reinforcing optimization cycle. The optimization cycle incorporates three key components, i.e., dynamic controllable filtering, iterative labeled dataset construction, and Bayes-optimal classifier construction. We present their details in the following paragraphs.

Dynamic controllable filtering to identify reliable pseudo-labels. Conventional SSL and LTSSL methods typically generate pseudo-labels by propagating predictions from weak augmentation views to their strong augmentation views. Although this strategy improves model robustness, it inherently introduces more error pseudo-labels when handling the unknown arbitrary unlabeled data distribution, as evidenced in Figs. 1(a) and 1(b). To overcome these limitations, we propose to identify reliable pseudo-labels to extend the labeled dataset instead of enforcing prediction consistency between weak and strong augmentation views. For each unlabeled sample x_u with weak augmentation view $\Omega_w(x_u)$ and strong augmentation view $\Omega_s(x_u)$, we derive predicted pseudo-labels and corresponding confidence scores as:

$$\begin{aligned}\hat{q}_w, \tilde{q}_w &= \arg \max(\sigma(f(h_w))), \max(\sigma(f(h_w))), \\ \hat{q}_s, \tilde{q}_s &= \arg \max(\sigma(f(h_s))), \max(\sigma(f(h_s))),\end{aligned}\quad (2)$$

where $\arg \max(\cdot)$ and $\max(\cdot)$ extract the pseudo-labels and confidence scores, respectively, and $\sigma(\cdot)$ denotes the softmax function. Let $h_w = g(\Omega_w(x_u))$ represent the representation produced by $g(\cdot)$ from $\Omega_w(x_u)$, with \hat{q}_w and \tilde{q}_w denoting the pseudo-label and its associated confidence score predicted for h_w , respectively. h_s , \hat{q}_s , and \tilde{q}_s are defined similarly for $\Omega_s(x_u)$. We express the binary sample mask for selecting a reliable pseudo-label as:

$$\mathbb{I} = \mathbb{I}(\tilde{q}_w > \tau) \cdot \mathbb{I}(\tilde{q}_s > \tau) \cdot \mathbb{I}(\hat{q}_w = \hat{q}_s), \quad (3)$$

where τ denotes the confidence threshold and \cdot represents element-wise multiplication. Since samples may receive conflicting pseudo-labels across different training steps according to Eq. (3), we introduce a voting strategy to ensure consistent pseudo-label assignments for each sample. As illustrated in Fig. 1(c), the combination of Eq. (3) and the voting strategy effectively controls pseudo-label generation and enhances pseudo-label reliability, demonstrating its strong performance.

Iterative labeled dataset construction. During the training process, we maintain both a labeled dataset and a pseudo-labeled dataset (i.e., identified reliable pseudo-labels) at each training step, with class frequencies denoted by $n = \{n_1, \dots, n_C\}$ and $m = \{m_1, \dots, m_C\}$, respectively. The updated labeled dataset's class frequency is defined as $\phi = \{\phi_1, \dots, \phi_C\}$, where $\phi_c = n_c + m_c$ denotes the number of samples for class c in the updated labeled dataset. Accordingly, the class distribution for the updated labeled dataset is given by:

$$\pi = \{\pi_1, \dots, \pi_C\}, \pi_c = \frac{\phi_c}{\sum_{c' \in [C]} \phi_{c'}}, \quad (4)$$

where π_c represents the label frequency of the c -th class in the updated labeled dataset. This yields an updated labeled dataset with a known distribution at each training step, enabling the iterative construction of a Bayes-optimal classifier.

Bayes-optimal classifier construction. Leveraging the known distribution of the updated labeled dataset, we construct a classifier by minimizing the LA loss (ℓ_{la}) defined in Eq. (1). The resulting classifier minimizes the balanced error and yields Bayes-optimal predictions [16]. By iteratively

constructing a Bayes-optimal classifier using the updated labeled dataset (with a known distribution at each training step), our CPG framework generates increasingly reliable pseudo-labels in subsequent training steps. Although our method does not explicitly estimate the unlabeled data distribution, the progressive incorporation of reliable pseudo-labels naturally approximates the ground-truth unlabeled data distribution as training progresses. This is because the model’s increasing confidence enables it to gradually include more diverse samples, including those from minority classes, improving distribution alignment (as demonstrated in Appendix A Fig. 5).

While consistency regularization between augmentation views is commonly used in SSL, we avoid it in our controllable self-reinforcing optimization cycle for two key reasons. First, pseudo-label quality is highly sensitive to the distribution mismatch between labeled and unlabeled data in LTSSL. Second, propagating error pseudo-labels from weak augmentation views to strong augmentation views can reinforce the model’s learning of incorrect predictions, leading to error accumulation and performance degradation (as demonstrated in Figs. 1 and 3).

Class-aware adaptive augmentation to enhance minority class representations. While the controllable self-reinforcing optimization cycle effectively utilizes unlabeled samples with reliable pseudo-labels and iteratively constructs Bayes-optimal classifiers, enhancing discriminative representations for minority classes remains crucial in long-tailed learning. To achieve this goal, we enhance the updated labeled dataset by synthesizing minority class representations guided by class compactness. Formally, the compactness of class c is defined as:

$$\alpha(c) = \frac{1}{\phi_c} \sum_{i \in [\phi_c]} \frac{\langle h_i, \mu(c) \rangle}{\|h_i\| \cdot \|\mu(c)\|}, \quad (5)$$

where ϕ_c denotes the number of samples in class c , $h_i = g(x_i)$ denotes the representation produced by encoder $g(\cdot)$, $\mu(c)$ denotes the centroid of class c in the feature space, and $\|\cdot\|$ denotes the Euclidean norm. As minority classes typically exhibit lower intra-class diversity, it is associated with a higher compactness α according to Eq. (5) and benefits from representation synthesis with a smaller augmentation radius r to refine decision boundaries, where $r = 1/\alpha$. The representation synthesis for sample x_i from minority class c is computed as:

$$h'_i = h_i + \frac{h_i}{\|h_i\|} \cdot r(c) \cdot \delta_i, \quad (6)$$

where δ_i is a noise vector sampled from a d -dimensional standard normal distribution (with d matching the representation dimension). For minority classes in the updated labeled dataset, we synthesize ten augmented representations per original sample by Eq. (6).

Auxiliary branch to maximize data utilization. Our controllable self-reinforcing optimization cycle incorporates reliable pseudo-labels from the unlabeled dataset into the labeled dataset and trains the model on the updated labeled dataset. However, during early training stages when model performance is still weak, only a limited number of samples meet the reliability condition for pseudo-labeling (as demonstrated in Figs. 1 and 3, and Appendix A Fig. 5). To maximize data utilization and provide additional supervision signals to stabilize representation learning during the critical initial phase, we introduce an auxiliary branch to leverage all labeled and unlabeled samples. Specifically, this branch adopts a consistency regularization paradigm similar to the conventional SSL methods like FixMatch [7], enforcing prediction consistency between weak and strong augmentation views via an unsupervised consistency regularization loss (Aux loss, ℓ_{aux}). The Aux loss ℓ_{aux} is formulated as:

$$\ell_{aux} = -\log \frac{e^{f_{\hat{y}}(g(x))}}{\sum_{y' \in [C]} e^{f_{y'}(g(x))}}, \quad (7)$$

where $f_{\hat{y}}(g(x))$ denotes the logit produced by the strong augmentation view, corresponding to the pseudo-label \hat{y} generated from the weak augmentation view.

3.3 Model Training and Prediction

Our training process consists of an initial stage of thirty epochs using only the labeled dataset, followed by an iterative stage that expands the labeled dataset with reliable pseudo-labels and continues optimization on the updated labeled dataset. Throughout both stages, the auxiliary branch is trained on all labeled and unlabeled samples. We optimize the model by combining the LA loss (ℓ_{la}) applied to both branches, with the Aux loss (ℓ_{aux}) applied only to the auxiliary branch. The overall loss $\ell_{overall}$ is formulated as:

Algorithm 1 Training process of our CPG

```

1: Input: Labeled and unlabeled datasets  $\mathcal{D}_l$  and  $\mathcal{D}_u$ .
2: Output: Encoder  $g$ , primary branch (classifier)  $f_{pri}$ , and auxiliary branch (classifier)  $f_{aux}$ .
3: Initialize the parameters of  $g$ ,  $f_{pri}$ , and  $f_{aux}$  randomly.
4: for epoch=1, 2, ... do
5:   for batch=1, 2, ... do
6:     if epoch > 30 then
7:       Identify reliable pseudo-labels by Eq. (2) and Eq. (3);
8:       Calculate the class distribution of the updated labeled dataset by Eq. (4);
9:       Enhance minority class representations by Eq. (5) and Eq. (6);
10:      end if
11:      Calculate the LA loss by Eq. (1) for the primary branch;
12:      Calculate the LA loss by Eq. (1) and Aux loss by Eq. (7) for the auxiliary branch;
13:      Obtain the overall loss by Eq. (8);
14:      Update network parameters via gradient descent;
15:    end for
16:  end for

```

$$\ell_{overall} = \ell_{la} + \omega \ell_{aux}, \quad (8)$$

where ω is a binary indicator function that equals 1 when $\ell_{overall}$ is applied to the auxiliary branch and 0 otherwise. The pseudo-code is detailed in Algorithm 1. After training, we can obtain the predicted label of an unseen sample x^* by getting the label index with the highest confidence.

3.4 Theoretical Analysis

We prove that our controllable self-reinforcing optimization cycle (including progressively incorporating reliable pseudo-labels into the labeled dataset and training a Bayes-optimal classifier on the updated labeled dataset with a known distribution) can significantly reduce the generalization error under some conditions. Let $\ell_{ours} = \frac{1}{N+\hat{M}_t} \left[\sum_{i=1}^N \ell_{la}(f(x_i), y_i) + \sum_{j=1}^{\hat{M}_t} \ell_{la}(f(x_j), \hat{y}_j) \right]$ be the training loss on the N labeled and \hat{M}_t pseudo-labeled samples with pseudo-labeling error rate ϵ_t for our method at the t -th training step. We begin by defining the model empirical risk R at the t -th training step as:

$$R_t = R_{t-1} - \lambda_t + I_{\epsilon_t} + I_{O_t}, \quad (9)$$

where R_t denotes the model empirical risk at the t -th training step, $\lambda_t \geq 0$ quantifies the empirical risk reduction achieved, and I_{ϵ_t} and I_{O_t} represent the impact of noisy pseudo-labels and number of training samples, respectively. Let the function space \mathcal{H}_y for the label $y \in \{1, \dots, C\}$ be $\{h : x \mapsto f_y(x) | f \in \mathcal{F}\}$, where $f_y(x)$ denotes the predicted probability of the y -th class. Let $\mathcal{R}_{O_t}(\mathcal{H}_y)$ be the expected Rademacher complexity [38] of \mathcal{H}_y with $O_t = N + \hat{M}_t$ training samples. Then we have the following theorem.

Theorem 1 (Generalization Error). *Suppose that the loss function $\ell_{la}(f(x), y)$ is ρ -Lipschitz with respect to $f(x)$ for all $y \in \{1, \dots, C\}$ and upper-bounded by U . Given the pseudo-labeling error rate $0 < \epsilon < 1$, for any $v > 0$, with probability at least $1 - v$, we have:*

$$R_T \leq R_0 - \sum_{t=1}^T \lambda_t + U \sum_{t=1}^T \epsilon_t + 4\sqrt{2}\rho \sum_{t=1}^T \sum_{y=1}^C \mathcal{R}_{O_t}(\mathcal{H}_y) + 2U \sum_{t=1}^T \sqrt{\frac{\log \frac{2}{v}}{2O_t}}, \quad (10)$$

where T denotes the total number of training steps, R_T and R_0 represent the model empirical risk at the final training step and initial training step (without pseudo-labels), respectively, and ϵ_t represents the pseudo-labeling error rate at the t -th training step.

The proof of Theorem 1 is provided in Appendix B. It can be observed that the model empirical risk R_T depends primarily on three key factors, i.e., the cumulative model empirical risk reduction $\sum_{t=1}^T \lambda_t$, the cumulative pseudo-labeling error rate $\sum_{t=1}^T \epsilon_t$, and the number of training samples O_t at each training step. When the training step t increases, the number of training samples O_t grows while the pseudo-labeling error rate ϵ_t either decreases or remains constant, the Bayes-optimal

classifier constructed at the t -th training step can maximize the model empirical risk reduction λ_t , i.e., as $T \rightarrow \infty$, $O_T \rightarrow \infty$, $\sum_{t=1}^T \epsilon_t$ remains bounded, and $\sum_{t=1}^T \lambda_t$ reaches its theoretical maximum, Theorem 1 demonstrates that the generalization error is minimized. As shown in Figs. 3(a) and 3(b), our CPG framework demonstrates superior performance over baseline methods, achieving both: (i) a consistently lower pseudo-labeling error rate ϵ_t , and (ii) a growing number of training samples O_t that gradually match baseline levels during training. Together with the Bayes-optimal classifier, our CPG can significantly reduce the generalization error.

4 Experiments

4.1 Experimental setting

Dataset. We perform our experiments on four widely-used datasets (CIFAR-10-LT [39], CIFAR-100-LT [39], Food-101-LT [40], and SVHN-LT [41]), following the main experimental settings in FreeMatch [8] and SimPro [13]. More details about those datasets are provided in Appendix C, and implementation details are provided in Appendix D.

Baselines. We compare with three SSL algorithms, i.e., FixMatch [7], FreeMatch [8], and SoftMatch [9], and three recent ReaLTSSL algorithms, including ACR [14], SimPro [13], and CDMAD [42]. Moreover, we use the supervised learning (SL) setting as a performance upper-bound reference. For a fair comparison, we test these baselines and our CPG on the widely-used codebase USB². For the data augmentation strategy, an identical weak augmentation is applied to both labeled and unlabeled data, while reserving a strong augmentation for unlabeled data. We use the same dataset splits with no overlap between labeled and unlabeled training data for all datasets.

Table 1: Comparison of accuracy (%) on CIFAR-10-LT ($N_{max} = 400$, $M_{max} = 4600$) with class imbalance ratio $\gamma \in \{100, 150, 200\}$ under different unlabeled data distributions. CE and LA denote using softmax cross-entropy loss and logit-adjusted softmax cross-entropy loss under the supervised learning (SL) setting, respectively. \dagger indicates we reproduce ACR without anchor distributions for a fair comparison.

Scenario	Method	$\gamma = 100$			$\gamma = 150$			$\gamma = 200$			Avg.
		Arbitrary	Inverse	Consistent	Arbitrary	Inverse	Consistent	Arbitrary	Inverse	Consistent	
SL	CE	82.90 \pm 2.00	83.89 \pm 0.36	79.14 \pm 0.20	81.06 \pm 2.42	82.48 \pm 0.30	74.51 \pm 0.46	79.20 \pm 1.21	81.43 \pm 0.53	72.12 \pm 0.18	79.64 \pm 0.85
	LA [16]	87.00 \pm 0.65	86.84 \pm 0.36	85.92 \pm 0.14	85.61 \pm 0.96	85.59 \pm 0.09	83.88 \pm 0.55	84.55 \pm 0.71	85.02 \pm 0.38	82.56 \pm 0.22	85.22 \pm 0.45
SSL	FixMatch [7]	62.17 \pm 4.64	57.61 \pm 1.71	68.35 \pm 1.44	57.73 \pm 3.74	56.51 \pm 2.22	64.54 \pm 1.34	54.16 \pm 4.03	51.43 \pm 5.24	61.53 \pm 1.08	59.34 \pm 2.83
	FreetMatch [8]	65.41 \pm 3.93	68.91 \pm 1.78	70.08 \pm 0.67	63.35 \pm 4.84	66.69 \pm 2.77	63.47 \pm 2.30	62.35 \pm 6.30	64.31 \pm 4.44	59.53 \pm 1.50	64.90 \pm 3.17
ReaLTSSL	SoftMatch [9]	66.13 \pm 2.27	66.00 \pm 1.56	72.75 \pm 1.09	62.92 \pm 2.22	65.57 \pm 0.53	68.85 \pm 1.28	59.09 \pm 1.95	63.62 \pm 2.13	62.49 \pm 0.48	65.27 \pm 1.50
	ACR \dagger [14]	60.60 \pm 4.21	62.54 \pm 4.04	73.20 \pm 1.80	48.22 \pm 8.07	51.08 \pm 1.03	68.31 \pm 3.05	50.13 \pm 7.50	53.40 \pm 3.49	65.12 \pm 1.05	59.18 \pm 3.51
	SimPro [13]	65.81 \pm 1.60	63.70 \pm 1.50	64.13 \pm 2.03	61.41 \pm 8.10	61.27 \pm 0.72	62.32 \pm 2.41	59.11 \pm 8.49	58.09 \pm 3.74	59.31 \pm 3.11	61.68 \pm 3.52
	CDMAD [42]	63.39 \pm 1.34	60.24 \pm 3.13	64.63 \pm 1.57	59.45 \pm 1.17	61.44 \pm 1.11	65.29 \pm 0.93	56.39 \pm 2.45	58.68 \pm 3.90	59.38 \pm 1.85	60.99 \pm 1.94
Ours		82.10 \pm 0.74	82.37 \pm 0.15	76.93 \pm 2.68	76.38 \pm 3.87	78.19 \pm 1.63	70.75 \pm 2.13	75.18 \pm 3.28	77.45 \pm 1.44	68.33 \pm 3.94	76.41 \pm 2.21

Table 2: Comparison of accuracy (%) on CIFAR-100-LT ($N_{max} = 50$, $M_{max} = 450$) with class imbalance ratio $\gamma \in \{10, 15, 20\}$ under different unlabeled data distributions.

Scenario	Method	$\gamma = 10$			$\gamma = 15$			$\gamma = 20$			Avg.
		Arbitrary	Inverse	Consistent	Arbitrary	Inverse	Consistent	Arbitrary	Inverse	Consistent	
SL	CE	64.73 \pm 0.27	65.35 \pm 0.21	64.62 \pm 0.24	61.85 \pm 0.29	63.12 \pm 0.26	61.61 \pm 0.26	59.94 \pm 0.33	61.29 \pm 0.27	58.91 \pm 0.29	62.38 \pm 0.27
	LA [16]	66.83 \pm 0.33	66.68 \pm 0.18	66.50 \pm 0.28	64.52 \pm 0.47	64.89 \pm 0.25	63.80 \pm 0.21	62.73 \pm 0.38	63.44 \pm 0.30	62.22 \pm 0.35	64.62 \pm 0.30
SSL	FixMatch [7]	48.89 \pm 1.27	47.92 \pm 1.63	50.04 \pm 0.80	42.91 \pm 0.64	41.54 \pm 1.00	44.60 \pm 0.48	40.64 \pm 1.06	38.77 \pm 0.60	42.11 \pm 0.57	44.16 \pm 0.89
	FreetMatch [8]	45.97 \pm 0.57	45.74 \pm 1.35	46.36 \pm 0.93	40.66 \pm 0.62	40.68 \pm 0.48	41.08 \pm 0.26	38.05 \pm 0.12	39.24 \pm 0.27	39.61 \pm 0.80	41.93 \pm 0.60
ReaLTSSL	SoftMatch [9]	47.99 \pm 0.85	48.17 \pm 1.04	48.86 \pm 0.34	42.62 \pm 1.34	41.42 \pm 0.46	43.78 \pm 0.84	40.24 \pm 0.93	40.17 \pm 1.10	41.13 \pm 0.35	43.82 \pm 0.80
	ACR \dagger [14]	44.10 \pm 1.59	48.50 \pm 0.86	41.33 \pm 0.41	35.12 \pm 1.36	39.01 \pm 0.38	32.73 \pm 1.74	29.08 \pm 1.11	32.78 \pm 1.59	29.69 \pm 2.94	36.93 \pm 1.33
	SimPro [13]	44.26 \pm 0.57	44.14 \pm 1.12	45.67 \pm 0.88	39.00 \pm 0.50	37.00 \pm 0.39	41.32 \pm 0.80	35.57 \pm 1.11	34.35 \pm 0.63	37.86 \pm 0.65	39.91 \pm 0.74
	CDMAD [42]	33.95 \pm 2.94	35.02 \pm 1.62	37.15 \pm 0.95	31.36 \pm 1.55	29.60 \pm 0.47	32.62 \pm 4.81	28.89 \pm 5.23	25.18 \pm 1.68	28.37 \pm 1.58	31.35 \pm 2.72
Ours		51.48 \pm 0.32	51.46 \pm 0.22	51.22 \pm 0.71	46.26 \pm 1.40	47.88 \pm 0.24	45.94 \pm 1.02	44.17 \pm 1.30	44.17 \pm 1.01	42.66 \pm 0.56	47.25 \pm 0.75

4.2 Results

Consistent distribution settings. We begin our analysis by evaluating performance under the consistent distribution setting, where labeled and unlabeled data follow an identical long-tailed distribution. Tables 1 and 2 present the primary results for CIFAR-10-LT and CIFAR-100-LT, respectively. Across all imbalance ratios, CPG achieves superior classification accuracy compared to previous baselines. For example, given $(N_{max}, M_{max}, \gamma) = (400, 4600, 100)$, CPG outperforms all baselines by up to 3.73 percentage points (pp) on CIFAR-10-LT. Similar improvements are observed for Food-101-LT and SVHN-LT in Table 3. On Food-101-LT with $(N_{max}, M_{max}, \gamma) = (50, 450, 15)$, CPG achieves gains of up to 2.27 pp.

²<https://github.com/microsoft/Semi-supervised-learning>

Table 3: Comparison of accuracy (%) on Food-101-LT ($N_{max} = 50, M_{max} = 450$) with class imbalance ratio $\gamma \in \{10, 15\}$ and SVHN-LT ($N_{max} = 400, M_{max} = 4600, \gamma = 100$) under different unlabeled data distributions.

Scenario	Method	Food-101-LT						Avg.	SVHN-LT			Avg.	
		$\gamma = 10$			$\gamma = 15$				Arbitrary	Inverse	Consistent		
		Arbitrary	Inverse	Consistent	Arbitrary	Inverse	Consistent		Arbitrary	Inverse	Consistent		
SL	CE	48.51 \pm 0.73	49.44 \pm 0.41	47.92 \pm 0.35	45.45 \pm 1.16	46.40 \pm 0.08	44.58 \pm 0.29	47.05 \pm 0.50	91.58 \pm 0.60	92.19 \pm 0.29	91.92 \pm 0.10	91.90 \pm 0.33	
	LA [16]	50.56 \pm 0.26	50.60 \pm 0.30	50.06 \pm 0.35	47.78 \pm 0.75	48.32 \pm 0.16	47.36 \pm 0.25	49.11 \pm 0.35	93.26 \pm 0.90	94.37 \pm 0.09	92.13 \pm 0.40	93.25 \pm 0.46	
SSL	FixMatch [7]	22.28 \pm 0.88	21.18 \pm 0.30	23.37 \pm 0.49	18.46 \pm 1.07	17.47 \pm 0.40	19.77 \pm 0.24	20.42 \pm 0.56	89.57 \pm 2.34	87.29 \pm 0.37	93.13 \pm 0.04	90.00 \pm 0.92	
	FretMatch [8]	22.28 \pm 1.12	21.89 \pm 0.87	22.22 \pm 0.68	18.72 \pm 0.80	18.66 \pm 0.46	19.61 \pm 0.38	20.56 \pm 0.72	85.78 \pm 2.87	87.01 \pm 1.56	90.88 \pm 0.48	87.89 \pm 1.64	
	SoftMatch [9]	22.87 \pm 0.76	22.30 \pm 0.73	22.72 \pm 0.75	19.46 \pm 1.04	19.43 \pm 0.87	19.84 \pm 0.94	21.10 \pm 0.85	85.71 \pm 1.87	87.79 \pm 1.15	91.07 \pm 0.42	88.19 \pm 1.15	
RealTSSL	ACR \dagger [14]	18.41 \pm 0.75	19.27 \pm 1.12	17.30 \pm 0.58	15.44 \pm 0.50	17.07 \pm 0.61	13.88 \pm 0.73	16.90 \pm 0.72	87.67 \pm 4.60	84.20 \pm 1.58	92.64 \pm 0.50	88.17 \pm 2.23	
	SimPro [13]	19.59 \pm 0.77	17.31 \pm 0.50	21.34 \pm 0.41	15.29 \pm 0.93	14.51 \pm 0.72	17.63 \pm 0.42	17.61 \pm 0.63	90.10 \pm 2.75	88.50 \pm 0.12	86.55 \pm 4.32	88.38 \pm 2.40	
	CDMAD [42]	10.11 \pm 1.63	11.26 \pm 1.57	12.24 \pm 1.09	10.21 \pm 1.43	8.65 \pm 1.60	11.18 \pm 1.64	10.61 \pm 1.49	81.90 \pm 1.81	81.39 \pm 3.46	87.88 \pm 3.92	83.72 \pm 3.06	
Ours		25.98 \pm 0.66	25.52 \pm 0.43	25.24 \pm 0.30	21.88 \pm 0.85	21.27 \pm 0.51	22.11 \pm 0.72	23.67 \pm 0.58	93.99 \pm 0.34	94.74 \pm 0.49	93.45 \pm 0.52	94.06 \pm 0.45	

Inconsistent distribution settings. To assess the real-world scenarios with mismatched distributions, we evaluate CPG under inverse long-tailed and arbitrary unlabeled data distributions. As shown in Tables 1 and 2, CPG consistently surpasses baselines on both CIFAR-10-LT and CIFAR-100-LT. Notably, for $(N_{max}, M_{max}, \gamma) = (400, 4600, 100)$ with arbitrary unlabeled data distribution, CPG achieves performance gains of **15.97 pp** over existing methods on CIFAR-10-LT. For realistic benchmark Food-101-LT in Table 3, CPG outperforms all competitors by up to 3.22 pp given the setting $(N_{max}, M_{max}, \gamma) = (50, 450, 10)$ with inverse long-tailed unlabeled data distribution.

When evaluating the overall performance, our CPG framework consistently outperforms baselines across all datasets. Notably, it achieves an average accuracy improvement of **11.14 pp** on CIFAR-10-LT, 3.09 pp on CIFAR-100-LT, and 4.06 pp on SVHN-LT. Moreover, it maintains a significant gain of 2.57 pp on the challenging realistic benchmark Food-101-LT.

Note that we observe a less significant performance improvement on CIFAR-100-LT than on CIFAR-10-LT. This can be attributed to the inherent challenges of CIFAR-100. Although CIFAR-100 and CIFAR-10 have the same total training set size, CIFAR-100 divides the data into 100 fine-grained classes (compared to 10 in CIFAR-10), reducing per-class samples by an order of magnitude. The finer class granularity also increases inter-class similarity, making classification inherently more challenging. As a result, the upper-bound performance (e.g., supervised learning) on CIFAR-100-LT (64.62 pp) is significantly lower than on CIFAR-10-LT (85.22 pp). Moreover, our method leverages consistency regularization to enhance model stability and prevent severe performance degradation, maintaining a relatively stable lower-bound performance. The narrower gap between this lower bound and the constrained upper bound on CIFAR-100-LT inherently limits the absolute performance gains. Despite this, our method still achieves a substantial average accuracy improvement of 3.09 pp on CIFAR-100-LT, as detailed in Table 2.

4.3 Analysis

Evaluation under varying imbalance ratios.

Fig. 4 illustrates the performance of CPG across different unlabeled data imbalance ratios, where the labeled data distribution is long-tailed with a fixed imbalance ratio and the unlabeled data distribution is arbitrary with varying imbalance ratios. The datasets are CIFAR-10-LT with $(\gamma_l = 100, \gamma_u \in \{100, 150, 200, 250\})$ and CIFAR-100-LT with $(\gamma_l = 10, \gamma_u \in \{5, 10, 15, 20\})$. The results consistently indicate that our method outperforms previous baselines. Moreover, as the unlabeled data imbalance ratio increases, the performance of baseline methods degrades significantly. In contrast, our method maintains nearly consistent performance on CIFAR-10-LT and exhibits only minor degradation on CIFAR-100-LT, demonstrating robust performance across varying unlabeled data imbalance ratios.

Evaluation under arbitrary labeled data distribution. Real-world scenarios often exhibit dynamic distribution shifts where any class can become dominant, affecting both labeled and unlabeled data. While existing evaluations assume static long-tailed distributions for labeled data, we assess

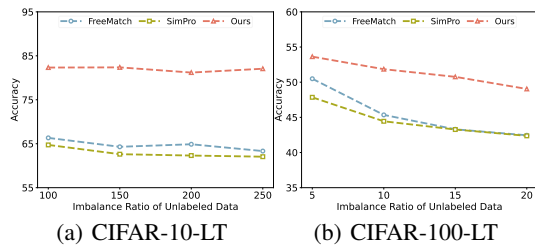


Figure 4: Comparison of accuracy (%) among FreeMatch [8], SimPro [13], and our CPG on CIFAR-10-LT and CIFAR-100-LT under arbitrary unlabeled data distribution with long-tailed labeled data distribution.

CPG under arbitrary labeled data distributions, with unlabeled data following either a consistent or inconsistent distribution relative to labeled data. As shown in Table 4, CPG consistently outperforms baselines on CIFAR-10-LT and CIFAR-100-LT, demonstrating exceptional robustness. For instance, with $(N_{max}, M_{max}, \gamma) = (400, 4600, 100)$ and an inconsistent unlabeled data distribution, CPG achieves performance gains of **11.82 pp** over existing methods on CIFAR-10-LT.

Ablation study. We conduct ablation studies to validate the effectiveness of key components in our CPG in Table 5. Specifically, we set $(N_{max}, M_{max}, \gamma) = (400, 4600, 100)$ for CIFAR-10-LT and $(N_{max}, M_{max}, \gamma) = (50, 450, 10)$ for CIFAR-100-LT, respectively. As shown in Table 5, we can observe that **each component brings a significant improvement**. For example, on CIFAR-10-LT, the auxiliary branch (AB) brings a performance gain of 0.80 pp given the arbitrary unlabeled data distribution. Moreover, class-aware adaptive augmentation (CAA) module further boosts performance by 2.99 pp over the AB baseline, while controllable self-reinforcing optimization cycle (CSOC) delivers a more substantial gain of **14.41 pp**. Combining CAA and CSOC achieves a synergistic improvement of **14.82 pp**, underscoring the complementary roles of these components. When evaluating the overall performance, CAA and CSOC individually contribute average performance gains of 2.35 pp and 6.97 pp, respectively, while their combination yields a **10.65 pp** improvement, reinforcing the effectiveness and robustness of our design.

Statistical significance. Table 6 presents the win/tie/loss counts between our CPG and six baseline methods across different datasets under varying unlabeled data distributions, using a pairwise t-test at a 0.05 significance level. The results show that our CPG outperforms baseline methods in all cases, with a significant improvement in 80.25 pp of cases (130 out of 162), demonstrating its effectiveness.

More experiment results and ablation studies are provided in Appendix E and Appendix F, respectively.

5 Conclusion

In this work, we have presented a novel solution to the ReaLTSSL problem via controllable pseudo-label generation. We proposed to expand the labeled dataset with reliable pseudo-labels and train the model on the updated labeled dataset with a known distribution, making it unaffected by the unlabeled data distribution. Our framework introduces a controllable self-reinforcing optimization cycle, combining dynamic controllable filtering for reliable pseudo-label identifying with iterative Bayes-optimal classifier construction through logit adjustment. It is further enhanced by a class-aware adaptive augmentation module for minority class representation learning and an auxiliary branch to maximize data utilization by leveraging all labeled and unlabeled samples. We further theoretically proved that this optimization cycle can significantly reduce the generalization error under some conditions. Comprehensive experiments on four commonly used benchmarks show consistent improvements of our method over the state-of-the-art methods by up to **15.97%** across various scenarios.

Table 4: Comparison of accuracy (%) on CIFAR-10-LT and CIFAR-100-LT under arbitrary labeled and unlabeled data distributions.

Scenario	Method	CIFAR-10-LT		CIFAR-100-LT	
		$(N_{max}, M_{max}, \gamma) = (400, 4600, 100)$	$(N_{max}, M_{max}, \gamma) = (50, 450, 10)$	Inconsistent	Consistent
SL	CE	82.90 \pm 3.34	78.48 \pm 4.61	64.75 \pm 0.58	63.77 \pm 0.31
	LA [16]	87.22 \pm 1.29	85.11 \pm 1.63	66.54 \pm 0.29	66.35 \pm 0.37
SSL	FixtMatch [7]	66.27 \pm 3.69	69.69 \pm 3.50	48.23 \pm 0.80	48.59 \pm 0.92
	FleetMatch [8]	62.02 \pm 2.21	69.73 \pm 2.80	45.59 \pm 0.31	46.49 \pm 0.78
	SoftMatch [9]	63.37 \pm 1.68	73.07 \pm 2.79	47.79 \pm 0.24	48.83 \pm 0.84
ReaLTSSL	ACR \dagger [14]	58.15 \pm 5.03	71.71 \pm 0.74	45.30 \pm 0.56	42.34 \pm 0.28
	SimPro [13]	70.40 \pm 5.18	67.54 \pm 2.31	44.10 \pm 0.45	45.82 \pm 1.53
	CDMAD [42]	60.26 \pm 0.26	66.45 \pm 2.89	32.86 \pm 5.85	35.79 \pm 3.22
	Ours	82.22 \pm 4.04	76.41 \pm 4.13	51.59 \pm 1.06	50.59 \pm 0.83

Table 5: Comparison of accuracy (%) on with and without the key components in the proposed method.

Ablations	CIFAR-10-LT			CIFAR-100-LT			Avg.	
	w/ AB	w/o AB	w/ CAA	w/o CAA	Arbitrary	Inverse	Consistent	
✓		65.18	63.94	66.10	46.32	46.23	45.84	55.60
✓		65.98	64.93	69.28	48.37	47.85	48.13	57.42 \uparrow 1.82
✓	✓	68.97	67.59	75.52	48.90	48.26	49.39	59.77 \uparrow 2.35
✓	✓	80.39	80.85	76.85	49.25	49.66	49.35	64.39 \uparrow 6.97
✓	✓	✓	82.33	82.32	78.35	51.85	51.61	51.04
								66.25 \uparrow 10.65

Table 6: Statistical significance of performance differences assessed with pairwise t-test at a 0.05 significance level, reported as win/tie/loss counts.

Scenario	Method	Arbitrary			Inverse			Consistent			Total
		1	2	3	1	2	3	1	2	3	
SSL	FixtMatch [7]	7	2	0	9	0	0	4	5	0	20 / 7 / 0
	FleetMatch [8]	9	0	0	9	0	0	7	2	0	25 / 2 / 0
	SoftMatch [9]	7	2	0	8	1	0	5	4	0	20 / 7 / 0
ReaLTSSL	ACR \dagger [14]	8	1	0	8	1	0	5	4	0	21 / 6 / 0
	SimPro [13]	6	3	0	9	0	0	7	2	0	22 / 5 / 0
	CDMAD [42]	8	1	0	9	0	0	5	4	0	22 / 5 / 0
	Total	45	9	0	52	2	0	33	21	0	130 / 32 / 0

References

- [1] Aibing Li, Xinyi Zeng, Pinxian Zeng, Sixian Ding, Peng Wang, Chengdi Wang, and Yan Wang. Textmatch: Using text prompts to improve semi-supervised medical image segmentation. In *Medical Image Computing and Computer Assisted Intervention (MICCAI)*, volume 15008, pages 699–709, 2024.
- [2] Lei Li, Sheng Lian, Zhiming Luo, Beizhan Wang, and Shaozi Li. Vclipseg: Voxel-wise clip-enhanced model for semi-supervised medical image segmentation. In *Medical Image Computing and Computer Assisted Intervention (MICCAI)*, volume 15009, pages 692–701, 2024.
- [3] Yaxiong Chen, Yujie Wang, Zixuan Zheng, Jingliang Hu, Yilei Shi, Shengwu Xiong, Xiao Xiang Zhu, and Lichao Mou. Striving for simplicity: Simple yet effective prior-aware pseudo-labeling for semi-supervised ultrasound image segmentation. In *Medical Image Computing and Computer Assisted Intervention (MICCAI)*, volume 15009, pages 604–614, 2024.
- [4] Dong-Hyun Lee. Pseudo-label: The simple and efficient semi-supervised learning method for deep neural networks. In *International Conference on Machine Learning (ICML)*, 2013.
- [5] Dongdong Chen, Wei Wang, Wei Gao, and Zhi-Hua Zhou. Tri-net for semi-supervised deep learning. In *Proceedings of the International Joint Conference on Artificial Intelligence (IJCAI)*, pages 2014–2020, 2018.
- [6] Paola Cascante-Bonilla, Fuwen Tan, Yanjun Qi, and Vicente Ordonez. Curriculum labeling: Revisiting pseudo-labeling for semi-supervised learning. In *Proceedings of the AAAI Conference on Artificial Intelligence*, volume 35, pages 6912–6920, 2021.
- [7] Kihyuk Sohn, David Berthelot, Nicholas Carlini, Zizhao Zhang, Han Zhang, Colin Raffel, Ekin Dogus Cubuk, Alexey Kurakin, and Chun-Liang Li. Fixmatch: Simplifying semi-supervised learning with consistency and confidence. In *Advances in Neural Information Processing Systems (NeurIPS)*, volume 33, pages 596–608, 2020.
- [8] Yidong Wang, Hao Chen, Qiang Heng, Wenxin Hou, Yue Fan, Zhen Wu, Jindong Wang, Marios Savvides, Takahiro Shinozaki, Bhiksha Raj, Bernt Schiele, and Xing Xie. Freematch: Self-adaptive thresholding for semi-supervised learning. In *International Conference on Learning Representations (ICLR)*, 2023.
- [9] Hao Chen, Ran Tao, Yue Fan, Yidong Wang, Jindong Wang, Bernt Schiele, Xing Xie, Bhiksha Raj, and Marios Savvides. Softmatch: Addressing the quantity-quality tradeoff in semi-supervised learning. In *International Conference on Learning Representations (ICLR)*, 2023.
- [10] Hyuck Lee, Seungjae Shin, and Heeyoung Kim. ABC: auxiliary balanced classifier for class-imbalanced semi-supervised learning. In *Advances in Neural Information Processing Systems (NeurIPS)*, volume 34, pages 7082–7094, 2021.
- [11] Yue Fan, Dengxin Dai, Anna Kukleva, and Bernt Schiele. Cossl: Co-learning of representation and classifier for imbalanced semi-supervised learning. In *IEEE/CVF Conference on Computer Vision and Pattern Recognition (CVPR)*, pages 14574–14584, 2022.
- [12] Qianhan Feng, Lujing Xie, Shijie Fang, and Tong Lin. Bacon: Boosting imbalanced semi-supervised learning via balanced feature-level contrastive learning. In *Proceedings of the AAAI Conference on Artificial Intelligence*, volume 38, pages 11970–11978, 2024.
- [13] Chaoqun Du, Yizeng Han, and Gao Huang. Simpro: A simple probabilistic framework towards realistic long-tailed semi-supervised learning. In *International Conference on Machine Learning (ICML)*, pages 11686–11703, 2024.
- [14] Tong Wei and Kai Gan. Towards realistic long-tailed semi-supervised learning: Consistency is all you need. In *IEEE/CVF Conference on Computer Vision and Pattern Recognition (CVPR)*, pages 3469–3478, 2023.
- [15] Chengcheng Ma, Ismail Elezi, Jiankang Deng, Weiming Dong, and Changsheng Xu. Three heads are better than one: Complementary experts for long-tailed semi-supervised learning. In *Proceedings of the AAAI Conference on Artificial Intelligence*, volume 38, pages 14229–14237, 2024.

[16] Aditya Krishna Menon, Sadeep Jayasumana, Ankit Singh Rawat, Himanshu Jain, Andreas Veit, and Sanjiv Kumar. Long-tail learning via logit adjustment. In *International Conference on Learning Representations (ICLR)*, 2021.

[17] Seulki Park, Youngkyu Hong, Byeongho Heo, Sangdoo Yun, and Jin Young Choi. The majority can help the minority: Context-rich minority oversampling for long-tailed classification. In *IEEE/CVF Conference on Computer Vision and Pattern Recognition (CVPR)*, pages 6887–6896, 2022.

[18] Jiang-Xin Shi, Tong Wei, Yuke Xiang, and Yufeng Li. How re-sampling helps for long-tail learning? In *Advances in Neural Information Processing Systems (NeurIPS)*, volume 36, pages 75669–75687, 2023.

[19] Qihao Zhao, Yalun Dai, Hao Li, Wei Hu, Fan Zhang, and Jun Liu. LTGC: long-tail recognition via leveraging llms-driven generated content. In *IEEE/CVF Conference on Computer Vision and Pattern Recognition (CVPR)*, pages 19510–19520, 2024.

[20] Yina He, Lei Peng, Yongcun Zhang, Juanjuan Weng, Shaozi Li, and Zhiming Luo. Long-tailed out-of-distribution detection: Prioritizing attention to tail. In *Proceedings of the AAAI Conference on Artificial Intelligence*, volume 39, pages 3446–3454, 2025.

[21] Yuchao Wang, Jingjing Fei, Haochen Wang, Wei Li, Tianpeng Bao, Liwei Wu, Rui Zhao, and Yujun Shen. Balancing logit variation for long-tailed semantic segmentation. In *IEEE/CVF Conference on Computer Vision and Pattern Recognition (CVPR)*, pages 19561–19573, 2023.

[22] Jiangpeng He. Gradient reweighting: Towards imbalanced class-incremental learning. In *IEEE/CVF Conference on Computer Vision and Pattern Recognition (CVPR)*, pages 16668–16677, 2024.

[23] Yanbiao Ma, Wei Dai, and Jiayi Chen. Pursuing better decision boundaries for long-tailed object detection via category information amount. In *International Conference on Learning Representations (ICLR)*, 2025.

[24] Xudong Wang, Long Lian, Zhongqi Miao, Ziwei Liu, and Stella X. Yu. Long-tailed recognition by routing diverse distribution-aware experts. In *International Conference on Learning Representations (ICLR)*, 2021.

[25] Emanuel Sanchez Aimar, Arvi Jonnarth, Michael Felsberg, and Marco Kuhlmann. Balanced product of calibrated experts for long-tailed recognition. In *IEEE/CVF Conference on Computer Vision and Pattern Recognition (CVPR)*, pages 19967–19977, 2023.

[26] Qihao Zhao, Chen Jiang, Wei Hu, Fan Zhang, and Jun Liu. MDCS: more diverse experts with consistency self-distillation for long-tailed recognition. In *IEEE/CVF International Conference on Computer Vision (ICCV)*, pages 11597–11608, 2023.

[27] Takeru Miyato, Shin-ichi Maeda, Masanori Koyama, and Shin Ishii. Virtual adversarial training: A regularization method for supervised and semi-supervised learning. *IEEE Transactions on Pattern Analysis and Machine Intelligence*, 41(8):1979–1993, 2019.

[28] Zhanghan Ke, Daoye Wang, Qiong Yan, Jimmy S. J. Ren, and Rynson W. H. Lau. Dual student: Breaking the limits of the teacher in semi-supervised learning. In *IEEE/CVF International Conference on Computer Vision (ICCV)*, pages 6728–6736, 2019.

[29] Bowen Zhang, Yidong Wang, Wenxin Hou, Hao Wu, Jindong Wang, Manabu Okumura, and Takahiro Shinozaki. Flexmatch: Boosting semi-supervised learning with curriculum pseudo labeling. In *Advances in Neural Information Processing Systems (NeurIPS)*, volume 34, pages 18408–18419, 2021.

[30] Siyuan Li, Weiyang Jin, Zedong Wang, Fang Wu, Zicheng Liu, Cheng Tan, and Stan Z. Li. Semireward: A general reward model for semi-supervised learning. In *International Conference on Learning Representations (ICLR)*, 2024.

[31] Chongsheng Zhang, Yixin Hou, Ke Chen, Shuang Cao, Gaojuan Fan, and Ji Liu. Quality-aware self-training on differentiable synthesis of rare relational data. In *Proceedings of the AAAI Conference on Artificial Intelligence*, volume 37, pages 6602–6611, 2023.

[32] Zhixin Li and Yuheng Jia. Commix: Contrastive mixup at representation level for long-tailed deep clustering. In *International Conference on Learning Representations (ICLR)*, 2025.

[33] Yuheng Jia, Xiaorui Peng, Ran Wang, and Min-Ling Zhang. Long-tailed partial label learning by head classifier and tail classifier cooperation. In *Proceedings of the AAAI Conference on Artificial Intelligence*, volume 38, pages 12857–12865, 2024.

[34] Yuhang Li, Zhuying Li, and Yuheng Jia. Boosting class representation via semantically related instances for robust long-tailed learning with noisy labels. In *IEEE/CVF International Conference on Computer Vision (ICCV)*, 2025.

[35] Yixin Hou, Weiping Ding, and Chongsheng Zhang. imftp: Deep imbalance learning via fuzzy transition and prototypical learning. *Information Sciences*, 679:121071, 2024.

[36] Chen Wei, Kihyuk Sohn, Clayton Mellina, Alan L. Yuille, and Fan Yang. Crest: A class-rebalancing self-training framework for imbalanced semi-supervised learning. In *IEEE/CVF Conference on Computer Vision and Pattern Recognition (CVPR)*, pages 10857–10866, 2021.

[37] Yixin Hou and Yuheng Jia. A square peg in a square hole: Meta-expert for long-tailed semi-supervised learning. In *International Conference on Machine Learning (ICML)*, 2025.

[38] Mehryar Mohri, Afshin Rostamizadeh, and Ameet Talwalkar. *Foundations of Machine Learning*. MIT Press, 2018.

[39] Alex Krizhevsky. Learning multiple layers of features from tiny images. <https://www.cs.toronto.edu/kriz/learning-features-2009-TR.pdf>, 2009.

[40] Lukas Bossard, Matthieu Guillaumin, and Luc Van Gool. Food-101 - mining discriminative components with random forests. In *European Conference on Computer Vision (ECCV)*, volume 8694, pages 446–461, 2014.

[41] Yuval Netzer, Tao Wang, Adam Coates, Alessandro Bissacco, Bo Wu, and Andrew Y. Ng. Reading digits in natural images with unsupervised feature learning. In *Advances in Neural Information Processing Systems (NeurIPS)*, 2011.

[42] Hyuck Lee and Heeyoung Kim. CDMAD: class-distribution-mismatch-aware debiasing for class-imbalanced semi-supervised learning. In *IEEE/CVF Conference on Computer Vision and Pattern Recognition (CVPR)*, pages 23891–23900, 2024.

[43] Andreas Maurer. A vector-contraction inequality for rademacher complexities. In *Algorithmic Learning Theory (ALT)*, volume 9925, pages 3–17, 2016.

[44] Sergey Zagoruyko and Nikos Komodakis. Wide residual networks. In *Proceedings of the British Machine Vision Conference (BMVC)*, 2016.

[45] Ilya Loshchilov and Frank Hutter. SGDR: stochastic gradient descent with warm restarts. In *International Conference on Learning Representations (ICLR)*, 2017.

[46] Wei-Ning Hsu, Benjamin Bolte, Yao-Hung Hubert Tsai, Kushal Lakhotia, Ruslan Salakhutdinov, and Abdelrahman Mohamed. Hubert: Self-supervised speech representation learning by masked prediction of hidden units. *IEEE/ACM Transactions on Audio, Speech, and Language Processing*, 29:3451–3460, 2021.

[47] Karol J. Piczak. ESC: dataset for environmental sound classification. In *Proceedings of the ACM Conference on Multimedia Conference*, pages 1015–1018, 2015.

[48] Mamshad Nayeem Rizve, Kevin Duarte, Yogesh S. Rawat, and Mubarak Shah. In defense of pseudo-labeling: An uncertainty-aware pseudo-label selection framework for semi-supervised learning. In *International Conference on Learning Representations (ICLR)*, 2021.

- [49] Xinting Hu, Yulei Niu, Chunyan Miao, Xian-Sheng Hua, and Hanwang Zhang. On non-random missing labels in semi-supervised learning. In *International Conference on Learning Representations (ICLR)*, 2022.
- [50] Emanuel Sanchez Aimar, Nathaniel Helgesen, Yonghao Xu, Marco Kuhlmann, and Michael Felsberg. Flexible distribution alignment: Towards long-tailed semi-supervised learning with proper calibration. In *European Conference on Computer Vision (ECCV)*, volume 15112, pages 307–327, 2024.
- [51] Youngtaek Oh, Dong-Jin Kim, and In So Kweon. DASO: distribution-aware semantics-oriented pseudo-label for imbalanced semi-supervised learning. In *IEEE/CVF Conference on Computer Vision and Pattern Recognition (CVPR)*, pages 9786–9796, 2022.
- [52] Yarin Gal and Zoubin Ghahramani. Dropout as a bayesian approximation: Representing model uncertainty in deep learning. In *International Conference on Machine Learning (ICML)*, pages 1050–1059, 2016.

NeurIPS Paper Checklist

1. Claims

Question: Do the main claims made in the abstract and introduction accurately reflect the paper's contributions and scope?

Answer: **[Yes]**

Justification: The main claims made in the abstract and introduction accurately reflect the paper's contributions and scope. Please see Abstract and Sec. 1.

Guidelines:

- The answer NA means that the abstract and introduction do not include the claims made in the paper.
- The abstract and/or introduction should clearly state the claims made, including the contributions made in the paper and important assumptions and limitations. A No or NA answer to this question will not be perceived well by the reviewers.
- The claims made should match theoretical and experimental results, and reflect how much the results can be expected to generalize to other settings.
- It is fine to include aspirational goals as motivation as long as it is clear that these goals are not attained by the paper.

2. Limitations

Question: Does the paper discuss the limitations of the work performed by the authors?

Answer: **[Yes]**

Justification: The paper discusses the limitations of the work performed by the authors. Please see Appendix H.

Guidelines:

- The answer NA means that the paper has no limitation while the answer No means that the paper has limitations, but those are not discussed in the paper.
- The authors are encouraged to create a separate "Limitations" section in their paper.
- The paper should point out any strong assumptions and how robust the results are to violations of these assumptions (e.g., independence assumptions, noiseless settings, model well-specification, asymptotic approximations only holding locally). The authors should reflect on how these assumptions might be violated in practice and what the implications would be.
- The authors should reflect on the scope of the claims made, e.g., if the approach was only tested on a few datasets or with a few runs. In general, empirical results often depend on implicit assumptions, which should be articulated.
- The authors should reflect on the factors that influence the performance of the approach. For example, a facial recognition algorithm may perform poorly when image resolution is low or images are taken in low lighting. Or a speech-to-text system might not be used reliably to provide closed captions for online lectures because it fails to handle technical jargon.
- The authors should discuss the computational efficiency of the proposed algorithms and how they scale with dataset size.
- If applicable, the authors should discuss possible limitations of their approach to address problems of privacy and fairness.
- While the authors might fear that complete honesty about limitations might be used by reviewers as grounds for rejection, a worse outcome might be that reviewers discover limitations that aren't acknowledged in the paper. The authors should use their best judgment and recognize that individual actions in favor of transparency play an important role in developing norms that preserve the integrity of the community. Reviewers will be specifically instructed to not penalize honesty concerning limitations.

3. Theory assumptions and proofs

Question: For each theoretical result, does the paper provide the full set of assumptions and a complete (and correct) proof?

Answer: [Yes]

Justification: For each theoretical result, the paper provides the full set of assumptions and a complete (and correct) proof. Please see Sec. 3.4 and Appendix B.

Guidelines:

- The answer NA means that the paper does not include theoretical results.
- All the theorems, formulas, and proofs in the paper should be numbered and cross-referenced.
- All assumptions should be clearly stated or referenced in the statement of any theorems.
- The proofs can either appear in the main paper or the supplemental material, but if they appear in the supplemental material, the authors are encouraged to provide a short proof sketch to provide intuition.
- Inversely, any informal proof provided in the core of the paper should be complemented by formal proofs provided in appendix or supplemental material.
- Theorems and Lemmas that the proof relies upon should be properly referenced.

4. Experimental result reproducibility

Question: Does the paper fully disclose all the information needed to reproduce the main experimental results of the paper to the extent that it affects the main claims and/or conclusions of the paper (regardless of whether the code and data are provided or not)?

Answer: [Yes]

Justification: The paper fully discloses all the information needed to reproduce the main experimental results of the paper to the extent that it affects the main claims and/or conclusions of the paper (regardless of whether the code and data are provided or not). Please see Sec. 4.1, Appendix C, and Appendix D.

Guidelines:

- The answer NA means that the paper does not include experiments.
- If the paper includes experiments, a No answer to this question will not be perceived well by the reviewers: Making the paper reproducible is important, regardless of whether the code and data are provided or not.
- If the contribution is a dataset and/or model, the authors should describe the steps taken to make their results reproducible or verifiable.
- Depending on the contribution, reproducibility can be accomplished in various ways. For example, if the contribution is a novel architecture, describing the architecture fully might suffice, or if the contribution is a specific model and empirical evaluation, it may be necessary to either make it possible for others to replicate the model with the same dataset, or provide access to the model. In general, releasing code and data is often one good way to accomplish this, but reproducibility can also be provided via detailed instructions for how to replicate the results, access to a hosted model (e.g., in the case of a large language model), releasing of a model checkpoint, or other means that are appropriate to the research performed.
- While NeurIPS does not require releasing code, the conference does require all submissions to provide some reasonable avenue for reproducibility, which may depend on the nature of the contribution. For example
 - (a) If the contribution is primarily a new algorithm, the paper should make it clear how to reproduce that algorithm.
 - (b) If the contribution is primarily a new model architecture, the paper should describe the architecture clearly and fully.
 - (c) If the contribution is a new model (e.g., a large language model), then there should either be a way to access this model for reproducing the results or a way to reproduce the model (e.g., with an open-source dataset or instructions for how to construct the dataset).
 - (d) We recognize that reproducibility may be tricky in some cases, in which case authors are welcome to describe the particular way they provide for reproducibility. In the case of closed-source models, it may be that access to the model is limited in some way (e.g., to registered users), but it should be possible for other researchers to have some path to reproducing or verifying the results.

5. Open access to data and code

Question: Does the paper provide open access to the data and code, with sufficient instructions to faithfully reproduce the main experimental results, as described in supplemental material?

Answer: [Yes]

Justification: The paper provides open access to the data and code, with sufficient instructions to faithfully reproduce the main experimental results, as described in supplemental material.

Guidelines:

- The answer NA means that paper does not include experiments requiring code.
- Please see the NeurIPS code and data submission guidelines (<https://nips.cc/public/guides/CodeSubmissionPolicy>) for more details.
- While we encourage the release of code and data, we understand that this might not be possible, so “No” is an acceptable answer. Papers cannot be rejected simply for not including code, unless this is central to the contribution (e.g., for a new open-source benchmark).
- The instructions should contain the exact command and environment needed to run to reproduce the results. See the NeurIPS code and data submission guidelines (<https://nips.cc/public/guides/CodeSubmissionPolicy>) for more details.
- The authors should provide instructions on data access and preparation, including how to access the raw data, preprocessed data, intermediate data, and generated data, etc.
- The authors should provide scripts to reproduce all experimental results for the new proposed method and baselines. If only a subset of experiments are reproducible, they should state which ones are omitted from the script and why.
- At submission time, to preserve anonymity, the authors should release anonymized versions (if applicable).
- Providing as much information as possible in supplemental material (appended to the paper) is recommended, but including URLs to data and code is permitted.

6. Experimental setting/details

Question: Does the paper specify all the training and test details (e.g., data splits, hyperparameters, how they were chosen, type of optimizer, etc.) necessary to understand the results?

Answer: [Yes]

Justification: The paper specifies all the training and test details (e.g., data splits, hyperparameters, how they were chosen, type of optimizer, etc.) necessary to understand the results. Please see Sec. 4.1, Appendix C, and Appendix D.

Guidelines:

- The answer NA means that the paper does not include experiments.
- The experimental setting should be presented in the core of the paper to a level of detail that is necessary to appreciate the results and make sense of them.
- The full details can be provided either with the code, in appendix, or as supplemental material.

7. Experiment statistical significance

Question: Does the paper report error bars suitably and correctly defined or other appropriate information about the statistical significance of the experiments?

Answer: [Yes]

Justification: The paper reports error bars suitably and correctly defined or other appropriate information about the statistical significance of the experiments. Please see Sec. 4.3.

Guidelines:

- The answer NA means that the paper does not include experiments.
- The authors should answer “Yes” if the results are accompanied by error bars, confidence intervals, or statistical significance tests, at least for the experiments that support the main claims of the paper.

- The factors of variability that the error bars are capturing should be clearly stated (for example, train/test split, initialization, random drawing of some parameter, or overall run with given experimental conditions).
- The method for calculating the error bars should be explained (closed form formula, call to a library function, bootstrap, etc.)
- The assumptions made should be given (e.g., Normally distributed errors).
- It should be clear whether the error bar is the standard deviation or the standard error of the mean.
- It is OK to report 1-sigma error bars, but one should state it. The authors should preferably report a 2-sigma error bar than state that they have a 96% CI, if the hypothesis of Normality of errors is not verified.
- For asymmetric distributions, the authors should be careful not to show in tables or figures symmetric error bars that would yield results that are out of range (e.g. negative error rates).
- If error bars are reported in tables or plots, The authors should explain in the text how they were calculated and reference the corresponding figures or tables in the text.

8. Experiments compute resources

Question: For each experiment, does the paper provide sufficient information on the computer resources (type of compute workers, memory, time of execution) needed to reproduce the experiments?

Answer: [\[Yes\]](#)

Justification: The paper provides sufficient information on the computer resources (type of compute workers, memory, time of execution) needed to reproduce the experiments. Please see Appendix I.

Guidelines:

- The answer NA means that the paper does not include experiments.
- The paper should indicate the type of compute workers CPU or GPU, internal cluster, or cloud provider, including relevant memory and storage.
- The paper should provide the amount of compute required for each of the individual experimental runs as well as estimate the total compute.
- The paper should disclose whether the full research project required more compute than the experiments reported in the paper (e.g., preliminary or failed experiments that didn't make it into the paper).

9. Code of ethics

Question: Does the research conducted in the paper conform, in every respect, with the NeurIPS Code of Ethics <https://neurips.cc/public/EthicsGuidelines>?

Answer: [\[Yes\]](#)

Justification: The research conducted in the paper conforms, in every respect, with the NeurIPS Code of Ethics <https://neurips.cc/public/EthicsGuidelines>.

Guidelines:

- The answer NA means that the authors have not reviewed the NeurIPS Code of Ethics.
- If the authors answer No, they should explain the special circumstances that require a deviation from the Code of Ethics.
- The authors should make sure to preserve anonymity (e.g., if there is a special consideration due to laws or regulations in their jurisdiction).

10. Broader impacts

Question: Does the paper discuss both potential positive societal impacts and negative societal impacts of the work performed?

Answer: [\[Yes\]](#)

Justification: The paper discusses both potential positive societal impacts and negative societal impacts of the work performed. Please see Appendix J.

Guidelines:

- The answer NA means that there is no societal impact of the work performed.
- If the authors answer NA or No, they should explain why their work has no societal impact or why the paper does not address societal impact.
- Examples of negative societal impacts include potential malicious or unintended uses (e.g., disinformation, generating fake profiles, surveillance), fairness considerations (e.g., deployment of technologies that could make decisions that unfairly impact specific groups), privacy considerations, and security considerations.
- The conference expects that many papers will be foundational research and not tied to particular applications, let alone deployments. However, if there is a direct path to any negative applications, the authors should point it out. For example, it is legitimate to point out that an improvement in the quality of generative models could be used to generate deepfakes for disinformation. On the other hand, it is not needed to point out that a generic algorithm for optimizing neural networks could enable people to train models that generate Deepfakes faster.
- The authors should consider possible harms that could arise when the technology is being used as intended and functioning correctly, harms that could arise when the technology is being used as intended but gives incorrect results, and harms following from (intentional or unintentional) misuse of the technology.
- If there are negative societal impacts, the authors could also discuss possible mitigation strategies (e.g., gated release of models, providing defenses in addition to attacks, mechanisms for monitoring misuse, mechanisms to monitor how a system learns from feedback over time, improving the efficiency and accessibility of ML).

11. Safeguards

Question: Does the paper describe safeguards that have been put in place for responsible release of data or models that have a high risk for misuse (e.g., pretrained language models, image generators, or scraped datasets)?

Answer: [NA]

Justification: Our research does not release data or models, so the paper has no such risks.

Guidelines:

- The answer NA means that the paper poses no such risks.
- Released models that have a high risk for misuse or dual-use should be released with necessary safeguards to allow for controlled use of the model, for example by requiring that users adhere to usage guidelines or restrictions to access the model or implementing safety filters.
- Datasets that have been scraped from the Internet could pose safety risks. The authors should describe how they avoided releasing unsafe images.
- We recognize that providing effective safeguards is challenging, and many papers do not require this, but we encourage authors to take this into account and make a best faith effort.

12. Licenses for existing assets

Question: Are the creators or original owners of assets (e.g., code, data, models), used in the paper, properly credited and are the license and terms of use explicitly mentioned and properly respected?

Answer: [Yes]

Justification: The creators or original owners of assets (e.g., code, data, models), used in the paper, are properly credited and are the license and terms of use explicitly mentioned and properly respected.

Guidelines:

- The answer NA means that the paper does not use existing assets.
- The authors should cite the original paper that produced the code package or dataset.
- The authors should state which version of the asset is used and, if possible, include a URL.

- The name of the license (e.g., CC-BY 4.0) should be included for each asset.
- For scraped data from a particular source (e.g., website), the copyright and terms of service of that source should be provided.
- If assets are released, the license, copyright information, and terms of use in the package should be provided. For popular datasets, paperswithcode.com/datasets has curated licenses for some datasets. Their licensing guide can help determine the license of a dataset.
- For existing datasets that are re-packaged, both the original license and the license of the derived asset (if it has changed) should be provided.
- If this information is not available online, the authors are encouraged to reach out to the asset's creators.

13. New assets

Question: Are new assets introduced in the paper well documented and is the documentation provided alongside the assets?

Answer: [NA]

Justification: The paper does not release new assets.

Guidelines:

- The answer NA means that the paper does not release new assets.
- Researchers should communicate the details of the dataset/code/model as part of their submissions via structured templates. This includes details about training, license, limitations, etc.
- The paper should discuss whether and how consent was obtained from people whose asset is used.
- At submission time, remember to anonymize your assets (if applicable). You can either create an anonymized URL or include an anonymized zip file.

14. Crowdsourcing and research with human subjects

Question: For crowdsourcing experiments and research with human subjects, does the paper include the full text of instructions given to participants and screenshots, if applicable, as well as details about compensation (if any)?

Answer: [NA]

Justification: The paper does not involve crowdsourcing nor research with human subjects.

Guidelines:

- The answer NA means that the paper does not involve crowdsourcing nor research with human subjects.
- Including this information in the supplemental material is fine, but if the main contribution of the paper involves human subjects, then as much detail as possible should be included in the main paper.
- According to the NeurIPS Code of Ethics, workers involved in data collection, curation, or other labor should be paid at least the minimum wage in the country of the data collector.

15. Institutional review board (IRB) approvals or equivalent for research with human subjects

Question: Does the paper describe potential risks incurred by study participants, whether such risks were disclosed to the subjects, and whether Institutional Review Board (IRB) approvals (or an equivalent approval/review based on the requirements of your country or institution) were obtained?

Answer: [NA]

Justification: The paper does not involve crowdsourcing nor research with human subjects.

Guidelines:

- The answer NA means that the paper does not involve crowdsourcing nor research with human subjects.

- Depending on the country in which research is conducted, IRB approval (or equivalent) may be required for any human subjects research. If you obtained IRB approval, you should clearly state this in the paper.
- We recognize that the procedures for this may vary significantly between institutions and locations, and we expect authors to adhere to the NeurIPS Code of Ethics and the guidelines for their institution.
- For initial submissions, do not include any information that would break anonymity (if applicable), such as the institution conducting the review.

16. Declaration of LLM usage

Question: Does the paper describe the usage of LLMs if it is an important, original, or non-standard component of the core methods in this research? Note that if the LLM is used only for writing, editing, or formatting purposes and does not impact the core methodology, scientific rigorousness, or originality of the research, declaration is not required.

Answer: [NA]

Justification: The core method development in this research does not involve LLMs as any important, original, or non-standard components.

Guidelines:

- The answer NA means that the core method development in this research does not involve LLMs as any important, original, or non-standard components.
- Please refer to our LLM policy (<https://neurips.cc/Conferences/2025/LLM>) for what should or should not be described.

Table of Contents for the Appendix

• A : Evolution of Pseudo-label Predictions	23
• B : Proof of Theorem 1	23
• C : Dataset Details	26
• D : Implementation Details	26
• E : More Experiment Results and Analyses	27
• E.1 : Comparison of Macro-F1 on CIFAR-10-LT and CIFAR-100-LT	27
• E.2 : Evaluation on Audio Modality	27
• E.3 : Evaluation under Noisy Scenarios	27
• E.4 : Evaluation on Large-scale and Realistic Datasets	28
• E.5 : Evaluation under Extreme Settings	28
• E.6 : Evaluation using Other Architectures	28
• F : More Ablation Studies and Analyses	28
• F.1 : Ablation Study on the Confidence Threshold	28
• F.2 : Ablation Study on the Auxiliary Branch	29
• F.3 : Ablation Study on the Anchor Distributions	30
• G : Relation to Existing Methods	30
• H : Limitations	31
• I : Compute Resources	31
• J : Broader Impacts	31

A Evolution of Pseudo-label Predictions

Fig. 5 shows the evolution of pseudo-label predictions of our method under the arbitrary unlabeled data distribution, evaluated on CIFAR-10-LT. From Fig. 5, we observe that our CPG progressively increases the utilization rate of pseudo-labels while maintaining the high accuracy. The predicted distribution gradually approximates the ground-truth unlabeled data distribution, and the Kullback-Leibler (KL) divergence between the predicted and ground-truth unlabeled data distributions decreases during training.

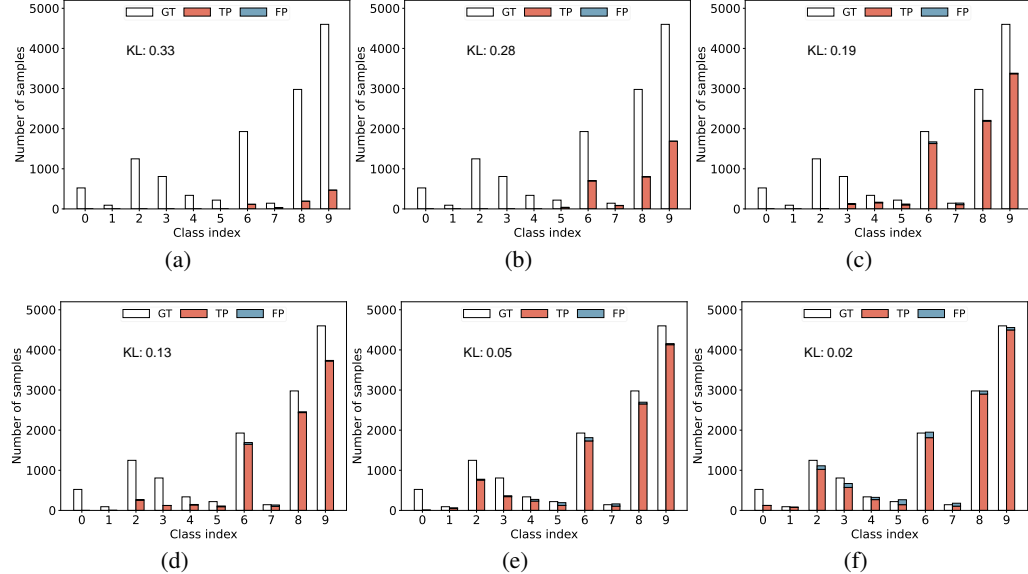


Figure 5: Evolution of pseudo-label predictions of our method under arbitrary unlabeled data distribution. GT denotes the ground-truth unlabeled data distribution. TP (FP) denotes the predicted true (false) positive pseudo-labels. KL denotes the Kullback-Leibler divergence between the predicted and ground-truth unlabeled data distributions. The dataset is CIFAR-10-LT with $(N_{max}, M_{max}, \gamma_l, \gamma_u) = (400, 4600, 50, 50)$. Our CPG can progressively increase the utilization rate of pseudo-labels while maintaining the high accuracy during training, as the pseudo-label distribution gradually approximates the ground-truth unlabeled data distribution.

B Proof of Theorem 1

We first copy the Theorem 1 here.

Theorem 1. Suppose that the loss function $\ell_{la}(f(x), y)$ is ρ -Lipschitz with respect to $f(x)$ for all $y \in \{1, \dots, C\}$ and upper-bounded by U . Given the pseudo-labeling error rate $0 < \epsilon < 1$, for any $v > 0$, with probability at least $1 - v$, we have:

$$R_T \leq R_0 - \sum_{t=1}^T \lambda_t + U \sum_{t=1}^T \epsilon_t + 4\sqrt{2}\rho \sum_{t=1}^T \sum_{y=1}^C \mathcal{R}_{O_t}(\mathcal{H}_y) + 2U \sum_{t=1}^T \sqrt{\frac{\log \frac{2}{v}}{2O_t}}, \quad (11)$$

where T denotes the total number of training steps, R_T and R_0 represent the model empirical risk at the final training step and initial training step (without pseudo-labels), respectively, and ϵ_t represents the pseudo-labeling error rate at the t -th training step.

Proof. We first restate the definition of the model empirical risk R at the t -th training step, i.e.,

$$R_t = R_{t-1} - \lambda_t + I_{\epsilon_t} + I_{O_t}, \quad (12)$$

where R_t denotes the model empirical risk at the t -th training step, $\lambda_t \geq 0$ quantifies the empirical risk reduction achieved, and I_{ϵ_t} and I_{O_t} represent the impact of noisy pseudo-labels and number of training samples, respectively. We derive I_{ϵ_t} and I_{O_t} below, omitting the subscript t for brevity.

We define the true risk on the training dataset with respect to the classification model $f(x; \theta)$ as:

$$R(f) = \mathbb{E}_{(x,y)} [\ell_{la}(f(x), y)]. \quad (13)$$

We aim to learn a good classification model by minimizing the empirical risk $\widehat{R}(f) = \widehat{R}_l(f) + \widehat{R}_u(f)$, with $\widehat{R}_l(f) = \frac{1}{N} \sum_{i=1}^N \ell_{la}(f(x_i), y_i)$ and $\widehat{R}_u(f) = \frac{1}{M} \sum_{j=1}^M \ell_{la}(f(x_j), y_j)$ representing the empirical risk on labeled and unlabeled training dataset, respectively.

Next, we derive the uniform deviation bound I_O between the true risk $R(f)$ and the empirical risk $\widehat{R}(f)$ using the following lemma.

Lemma 1. *Suppose that the loss function $\ell_{la}(f(x), y)$ is ρ -Lipschitz with respect to $f(x)$ for all $y \in \{1, \dots, C\}$ and upper-bounded by U . For any $v > 0$, with probability at least $1 - v$, we have:*

$$|R(f) - \widehat{R}(f)| \leq 2\sqrt{2}\rho \sum_{y=1}^C \mathcal{R}_{N+M}(\mathcal{H}_y) + U \sqrt{\frac{\log \frac{2}{v}}{2(N+M)}}, \quad (14)$$

where the function space \mathcal{H}_y for the label $y \in \{1, \dots, C\}$ is $\{h : x \mapsto f_y(x) | f \in \mathcal{F}\}$.

Proof. In order to prove this lemma, we define the Rademacher complexity of the composition of loss function ℓ_{la} and model $f \in \mathcal{F}$ with N labeled and M unlabeled training samples as follows:

$$\begin{aligned} & \mathcal{R}_{N+M}(\ell_{la} \circ \mathcal{F}) \\ &= \mathbb{E}_{(x,y,\mu)} \left[\sup_{f \in \mathcal{F}} \sum_{i=1}^N \mu_i \left(\ell_{la}(f(x_i), y_i) \right) + \sum_{j=1}^M \mu_j \left(\ell_{la}(f(x_j), y_j) \right) \right] \\ &\leq \sqrt{2}\rho \sum_{y=1}^C \mathcal{R}_{N+M}(\mathcal{H}_y), \end{aligned} \quad (15)$$

where \circ denotes the function composition operator, $\mathbb{E}_{(x,y,\mu)}$ denotes the expectation over x, y , and μ, μ denotes the Rademacher variable, $\sup_{f \in \mathcal{F}}$ denotes the supremum (or least upper bound) over the function set \mathcal{F} of model f . The second line holds because of the Rademacher vector contraction inequality [43].

Then, we proceed with the proof by showing that the one direction $\sup_{f \in \mathcal{F}} R(f) - \widehat{R}(f)$ is bounded with probability at least $1 - v/2$, and the other direction $\sup_{f \in \mathcal{F}} \widehat{R}(f) - R(f)$ can be proved similarly. Note that replacing a sample (x_i, y_i) leads to a change of $\sup_{f \in \mathcal{F}} R(f) - \widehat{R}(f)$ at most $\frac{U}{N+M}$ due to the fact that ℓ_{la} is bounded by U . According to the McDiarmid's inequality [38], for any $v > 0$, with probability at least $1 - v/2$, we have:

$$\sup_{f \in \mathcal{F}} R(f) - \widehat{R}(f) \leq \mathbb{E} \left[\sup_{f \in \mathcal{F}} R(f) - \widehat{R}(f) \right] + U \sqrt{\frac{\log \frac{2}{v}}{2(N+M)}}. \quad (16)$$

According to the result in [38] that shows $\mathbb{E} \left[\sup_{f \in \mathcal{F}} R(f) - \widehat{R}(f) \right] \leq 2\mathcal{R}_{N+M}(\mathcal{F})$, and further considering the other direction $\sup_{f \in \mathcal{F}} \widehat{R}(f) - R(f)$, with probability at least $1 - v$, we have:

$$\sup_{f \in \mathcal{F}} |R(f) - \widehat{R}(f)| \leq 2\sqrt{2}\rho \sum_{y=1}^C \mathcal{R}_{N+M}(\mathcal{H}_y) + U \sqrt{\frac{\log \frac{2}{v}}{2(N+M)}}, \quad (17)$$

which completes the proof. \square

In SSL, we cannot minimize the empirical risk $\widehat{R}_u(f)$ directly, since the ground-truth labels are inaccessible for unlabeled training data. Therefore, we need to train the model with $\widehat{R}'_u(f) =$

$\frac{1}{\hat{M}} \sum_{j=1}^{\hat{M}} \ell_{la}(f(x_j), \hat{y}_j)$, where \hat{y}_j denotes the pseudo-label of unlabeled sample x_j , and \hat{M} quantifies the pseudo-labels identified by the dynamic controllable filtering. Let $\hat{f} = \operatorname{argmin}_{f \in \mathcal{F}} \hat{R}(f)$ be the empirical risk minimizer, and $f^* = \operatorname{argmin}_{f \in \mathcal{F}} R(f)$ be the true risk minimizer. Let $\ell_{ours} = \frac{1}{N+\hat{M}} \left[\sum_{i=1}^N \ell_{la}(f(x_i), y_i) + \sum_{j=1}^{\hat{M}} \ell_{la}(f(x_j), \hat{y}_j) \right]$ be the training loss on N labeled and \hat{M} pseudo-labeled samples with pseudo-labeling error rate ϵ for our method.

Then, we can bound the difference I_{ϵ_t} between $\hat{R}_u(f)$ and $\hat{R}'_u(f)$ as follows.

Lemma 2. *Suppose that the loss function $\ell_{la}(f(x), y)$ is ρ -Lipschitz with respect to $f(x)$ for all $y \in \{1, \dots, C\}$ and upper-bounded by U . Given the pseudo-labeling error rate $0 < \epsilon < 1$, we have:*

$$0 \leq |\hat{R}'_u(f) - \hat{R}_u(f)| \leq U\epsilon. \quad (18)$$

Proof. Let's first expand $\hat{R}'_u(f)$:

$$\begin{aligned} \hat{R}'_u(f) &= \frac{1}{\hat{M}} \sum_{j=1}^{\hat{M}} \ell_{la}(f(x_j), \hat{y}_j) \\ &= \frac{1}{\hat{M}} \sum_{j=1}^{\hat{M}} \left[(1-\epsilon) \ell_{la}(f(x_j), y_j) + \frac{\epsilon}{C-1} \sum_{c=1}^C \mathbb{I}(\hat{y}_j \neq y_j) \ell_{la}(f(x_j), \hat{y}_j) \right]. \end{aligned} \quad (19)$$

Next, we show its upper bound:

$$\begin{aligned} \hat{R}'_u(f) &\leq \hat{R}_u(f) + \frac{1}{\hat{M}} \sum_{j=1}^{\hat{M}} \left[\frac{\epsilon}{C-1} \sum_{c=1}^C \mathbb{I}(\hat{y}_j \neq y_j) \ell_{la}(f(x_j), \hat{y}_j) \right] \\ &\leq \hat{R}_u(f) + \frac{1}{\hat{M}} \sum_{j=1}^{\hat{M}} \left[\frac{\epsilon}{C-1} \sum_{c=1}^C \mathbb{I}(\hat{y}_j \neq y_j) U \right] \\ &\leq \hat{R}_u(f) + U\epsilon, \end{aligned} \quad (20)$$

and when $\epsilon \rightarrow 0$, it reaches the lower bound $\hat{R}_u(f)$, which concludes the proof. \square

Based on the above lemmas, for any $v > 0$, with probability at least $1 - v$, at the t -th training step, we have:

$$\begin{aligned} R_t(\hat{f}) &\leq \hat{R}_t(\hat{f}) + 2\sqrt{2\rho} \sum_{y=1}^C \mathcal{R}_{O_t}(\mathcal{H}_y) + U \sqrt{\frac{\log \frac{2}{v}}{2O_t}} \\ &\leq \hat{R}_{t_l}(\hat{f}) + \hat{R}_{t_u}(\hat{f}) + 2\sqrt{2\rho} \sum_{y=1}^C \mathcal{R}_{O_t}(\mathcal{H}_y) + U \sqrt{\frac{\log \frac{2}{v}}{2O_t}} \\ &\leq \hat{R}_{t_l}(\hat{f}) + \hat{R}'_{t_u}(\hat{f}) + 2\sqrt{2\rho} \sum_{y=1}^C \mathcal{R}_{O_t}(\mathcal{H}_y) + U \sqrt{\frac{\log \frac{2}{v}}{2O_t}} \\ &\leq \hat{R}_{t_l}(f) + \hat{R}'_{t_u}(f) + 2\sqrt{2\rho} \sum_{y=1}^C \mathcal{R}_{O_t}(\mathcal{H}_y) + U \sqrt{\frac{\log \frac{2}{v}}{2O_t}} \\ &\leq \hat{R}_{t_l}(f) + \hat{R}_{t_u}(f) + U\epsilon_t + 2\sqrt{2\rho} \sum_{y=1}^C \mathcal{R}_{O_t}(\mathcal{H}_y) + U \sqrt{\frac{\log \frac{2}{v}}{2O_t}} \\ &\leq \hat{R}_t(f) + U\epsilon_t + 2\sqrt{2\rho} \sum_{y=1}^C \mathcal{R}_{O_t}(\mathcal{H}_y) + U \sqrt{\frac{\log \frac{2}{v}}{2O_t}} \end{aligned}$$

$$\leq R_t(f) + U\epsilon_t + 4\sqrt{2}\rho \sum_{y=1}^C \mathcal{R}_{O_t}(\mathcal{H}_y) + 2U\sqrt{\frac{\log \frac{2}{v}}{2O_t}}, \quad (21)$$

where the first and seventh lines are based on Lemma 1, and three and fifth lines are due to Lemma 2. The fourth line is by the definition of \hat{f} .

Then, we can derive $I_{\epsilon_t} + I_{O_t}$ as follows:

$$\begin{aligned} I_{\epsilon_t} + I_{O_t} &= |\hat{R}'_t(f) - \hat{R}_t(f)| + |R_t(f) - \hat{R}_t(f)| = |\hat{R}'_t(f) - R_t(f)| \\ &\leq U\epsilon_t + 4\sqrt{2}\rho \sum_{y=1}^C \mathcal{R}_{O_t}(\mathcal{H}_y) + 2U\sqrt{\frac{\log \frac{2}{v}}{2O_t}}, \end{aligned} \quad (22)$$

Substituting Eq. (22) into Eq. (12) yields:

$$\left\{ \begin{array}{l} R_t \leq R_{t-1} - \lambda_t + U\epsilon_t + 4\sqrt{2}\rho \sum_{y=1}^C \mathcal{R}_{O_t}(\mathcal{H}_y) + 2U\sqrt{\frac{\log \frac{2}{v}}{2O_t}}, \\ R_{t-1} \leq R_{t-2} - \lambda_{t-1} + U\epsilon_{t-1} + 4\sqrt{2}\rho \sum_{y=1}^C \mathcal{R}_{O_{t-1}}(\mathcal{H}_y) + 2U\sqrt{\frac{\log \frac{2}{v}}{2O_{t-1}}}, \\ \vdots \\ R_1 \leq R_0 - \lambda_1 + U\epsilon_1 + 4\sqrt{2}\rho \sum_{y=1}^C \mathcal{R}_{O_1}(\mathcal{H}_y) + 2U\sqrt{\frac{\log \frac{2}{v}}{2O_1}}. \end{array} \right. \quad (23)$$

Finally, combining the sub-equations in Eq. (23) through summation yields:

$$R_T \leq R_0 - \sum_{t=1}^T \lambda_t + U \sum_{t=1}^T \epsilon_t + 4\sqrt{2}\rho \sum_{t=1}^T \sum_{y=1}^C \mathcal{R}_{O_t}(\mathcal{H}_y) + 2U \sum_{t=1}^T \sqrt{\frac{\log \frac{2}{v}}{2O_t}}. \quad (24)$$

At this point, we have proven Theorem 1. □

C Dataset Details

We perform our experiments on four widely-used datasets (CIFAR-10-LT [39], CIFAR-100-LT [39], Food-101-LT [40], and SVHN-LT [41]), following the main experimental settings in FreeMatch [8] and SimPro [13], details are as below.

- *CIFAR-10-LT*: We test nine settings with $(N_{max}, M_{max}) = (400, 4600)$ and $\gamma \in \{100, 150, 200\}$. The unlabeled data follows either the same long-tailed distribution as the labeled data (consistent case), or an inverse long-tailed or arbitrary distribution (inconsistent cases).
- *CIFAR-100-LT*: We examine nine settings with $(N_{max}, M_{max}) = (50, 450)$ and $\gamma \in \{10, 15, 20\}$, using the same consistent/inconsistent unlabeled data distribution patterns as above.
- *Food-101-LT*: We evaluate six settings with $(N_{max}, M_{max}) = (50, 450)$ and $\gamma \in \{10, 15\}$, maintaining the same distribution cases.
- *SVHN-LT*: We evaluate three settings with $(N_{max}, M_{max}, \gamma) = (50, 450, 100)$, following the same distribution scheme.

D Implementation Details

We follow the default settings and hyperparameters in USB, i.e., the batch size of labeled data B_l is set to 64, while unlabeled data B_u is set to 7 times B_l , and the confidence threshold τ is set

to 0.95. Moreover, we use the WRN-28-2 [44] architecture, the SGD optimizer with momentum 0.9, and weight decay 5e-4 for training. We use a cosine learning rate decay [45] scheme, which sets the learning rate to $\eta \cos(\frac{7\pi t}{16T})$, where the initial learning rate η is set to 0.03, t is the current training step, and the total number of training steps T is set to 2^{18} . We repeat each experiment with three different random seeds (i.e., 0, 1, and 2) and report the mean and standard deviation of the performances. We conduct the experiments on a single NVIDIA RTX 4090 GPU using PyTorch v2.3.1.

E More Experiment Results and Analyses

E.1 Comparison of Macro-F1 on CIFAR-10-LT and CIFAR-100-LT

To better evaluate our method’s performance under class imbalance, we include the Macro-F1 metric in our analysis. Table 7 presents the results on CIFAR-10-LT and CIFAR-100-LT. In both cases, the labeled data follows a long-tailed distribution, while the unlabeled data varies across long-tailed, inverse long-tailed, and arbitrary distributions. The results in Table 7 show that our method achieves significant

improvements in Macro-F1 over existing baselines, further validating its effectiveness for imbalance learning. Notably, it yields average Macro-F1 gains of **13.84 pp** on CIFAR-10-LT and 4.55 pp on CIFAR-100-LT.

E.2 Evaluation on Audio Modality

While our method is evaluated on vision tasks, the core principles of CPG can be extended to other modalities. Here, we further evaluate our method on the audio modality. Specifically, for audio data, this adaptation requires two key modifications: (i) replacing vision-specific backbones (e.g., WRN-28-2 [44]) with audio-compatible models (e.g., HuBERT [46]), and (ii) substituting image augmentations with audio-specific ones. To demonstrate this adaptability, we perform our CPG on ESC-50-LT [47], a standard benchmark for environmental sound classification. As demonstrated in Table 8, our method achieves state-of-the-art performance on this audio benchmark, confirming its effectiveness beyond the visual modality. These results strongly support the generalizability of CPG’s framework across different modalities.

E.3 Evaluation under Noisy Scenarios

To comprehensively evaluate our method’s robustness under noisy scenarios, we conduct additional experiments on CIFAR-10-LT with ($N_{max} = 400, M_{max} = 4600, \gamma = 100$), under varying noise rates (i.e., 0%, 10%, 20%, and 30%). The labeled data follows a long-tailed distribution, while the unlabeled data adheres to an arbitrary distribution. As demonstrated in Table 9, our method consistently outperforms baselines in noisy settings, achieving the highest accuracy across all noise rates with minimal performance degradation. Notably, when noise rate increases from 0% to 30%, our method shows a degradation (Δ) of only 12.46

Table 7: Comparison of Macro-F1 (%) on CIFAR-10-LT ($N_{max} = 400, M_{max} = 4600, \gamma = 100$) and CIFAR-100-LT ($N_{max} = 50, M_{max} = 450, \gamma = 10$) under different unlabeled data distributions.

Scenario	Method	CIFAR-10-LT				CIFAR-100-LT				Avg.	
		$\gamma = 100$			Avg.			$\gamma = 10$			
		Arbitrary Inverse Consistent			Arbitrary Inverse Consistent						
SSL	FixMatch [7]	53.52	54.24	66.47	58.07	44.58	44.85	46.46	45.30		
	FreetMatch [8]	66.00	67.00	68.04	67.01	44.13	43.57	43.84	43.85		
	SoftMatch [9]	62.49	66.66	71.53	66.89	45.67	46.73	46.91	46.44		
ReaLTSSL	ACR† [14]	59.01	64.03	70.25	64.43	45.69	48.89	41.92	45.50		
	SimPro [13]	61.22	62.11	57.81	60.38	39.98	41.54	41.87	41.13		
	CDMAD [42]	61.73	62.88	62.11	62.24	32.97	35.80	36.68	35.15		
Ours		81.99	82.31	78.25	80.85	51.31	51.25	50.41	50.99		

Table 8: Comparison of accuracy (%) on ESC-50-LT ($N_{max} = 12, M_{max} = 12, \gamma = 1.2$) under long-tailed labeled data and arbitrary unlabeled data distributions.

FreeMatch [8]	SimPro [13]	Ours
68.13	68.75	69.13

Table 9: Comparison of accuracy (%) on CIFAR-10-LT ($N_{max} = 400, M_{max} = 4600, \gamma = 100$) across different noise rate scenarios.

Noise rate	0%	10%	20%	30%	$\Delta(0\% \rightarrow 30\%)$
FreetMatch [8]	66.33	60.33	56.24	51.29	-15.04
SimPro [13]	64.73	59.86	44.54	34.80	-29.93
Ours	82.33	75.95	71.82	69.87	-12.46

pp, compared to 15.04 pp for FreeMatch [8] and 29.93 pp for SimPro [13]. This demonstrates our method’s strong robustness to label noise.

E.4 Evaluation on Large-scale and Realistic Datasets

The Food-101 dataset (evaluated in Table 3) is a widely adopted benchmark for food image classification. Its training set naturally contains a proportion of label noise, making the data distribution implicitly unknown. Thus, distribution mismatches between labeled and unlabeled data occur when splitting the training set into labeled and unlabeled datasets. Despite these challenges, our method achieves a significant average accuracy gain of 2.57 pp on this dataset.

To further evaluate our method’s effectiveness in large-scale and real-world scenarios, we conduct experiments on ImageNet-127 (an imbalanced dataset, 127 classes, imbalance ratio 286) with an arbitrary (non-long-tailed) distribution. As shown in Table 10, our method consistently outperforms baselines, achieving gains of 1.27 pp at 32×32 resolution and 2.82 pp at 64×64 resolution. These results highlight our method’s robustness in large-scale and realistic settings beyond standard benchmarks.

E.5 Evaluation under Extreme Settings

In long-tailed learning scenarios, there exists an inherent trade-off between extremely small N_{max} (number of samples in the most frequent class) and large imbalance ratio γ values, since $N_{min} = N_{max}/\gamma \geq 1$. Our initial experiments on CIFAR-10-LT in Table 1 already employed challenging settings ($N_{max} = 400, M_{max} = 4600, \gamma = 100$) with $N_{min} = 4$. Notably, even with such extremely few tail class samples, our method still demonstrates significant performance gains over baselines.

To further evaluate our method, we conduct additional experiments under three more extreme settings: extreme sparsity setting A1 ($N_{max} = 100, N_{min} = 1, M_{max} = 4900, \gamma = 100$), extreme sparsity setting A2 ($N_{max} = 10, N_{min} = 1, M_{max} = 4990, \gamma_l = 10, \gamma_u = 300$), and extreme imbalance setting B ($N_{max} = 400, N_{min} = 1, M_{max} = 4600, \gamma = 300$). As demonstrated in Table 11, our method achieves state-of-the-art performance across three settings, attaining 69.56 pp in setting A1, 49.28 pp in setting A2, and 77.78 pp in setting B. These results represent significant improvements over all baseline methods, underscoring our method’s exceptional capability to handle extreme settings.

E.6 Evaluation using Other Architectures

To evaluate architectural generalization, we conduct experiments using ResNet-50 on CIFAR-10-LT with ($N_{max} = 400, M_{max} = 4600, \gamma = 100$). The labeled data follows a long-tailed distribution, while the unlabeled data conforms to either an inverse long-tailed or an arbitrary distribution. As evidenced by Table 12, our method demonstrates significant improvements, achieving absolute performance gains of 7.85 pp and 7.23 pp over current state-of-the-art methods in these respective scenarios. These results highlight our method’s consistent robustness when applied to different network architectures and its ability to handle varying distribution patterns in the unlabeled data.

Table 10: Comparison of accuracy (%) on ImageNet-127.

Scenario	Method	32×32	64×64
		29.57	37.40
SSL	FixMatch [7]	31.37	39.67
	FreetMatch [8]	31.50	39.40
	SoftMatch [9]		
ReaLTSSL	ACR† [14]	38.47	47.61
	SimPro [13]	43.31	46.93
	CDMAD [42]	15.46	21.92
	Ours	44.58	50.43

Table 11: Comparison of accuracy (%) on CIFAR-10-LT under extreme scenarios.

Method	Setting A1	Setting A2	Setting B1
FreetMatch [8]	63.86	45.75	55.92
SimPro [13]	31.01	15.20	50.98
Ours	69.56	49.28	77.78

Table 12: Comparison of accuracy (%) on CIFAR-10-LT using ResNet-50.

Method	Arbitrary	Inverse
FreetMatch [8]	47.68	48.28
SimPro [13]	43.67	51.26
Ours	55.53	58.49

F More Ablation Studies and Analyses

F.1 Ablation Study on the Confidence Threshold

The confidence threshold $\tau = 0.95$ is a common setting in SSL, which we adopt for a fair comparison. To evaluate the impact of different confidence thresholds on model performance, we conduct

additional experiments on CIFAR-10-LT with ($N_{max} = 400$, $M_{max} = 4600$, $\gamma_l = 100$) and $\tau \in \{0.75, 0.85, 0.95\}$. As shown in Table 13, our method's performance variations across different thresholds remain relatively small (within 1-2 pp), and it maintains consistently superior performance compared to baseline methods. This threshold-insensitive property highlights the stability of our method.

Table 13: Ablation study on the confidence threshold.

Method	Arbitrary	Inverse	Consistent
FreetMatch [8]	66.33	68.10	69.42
SimPro [13]	64.73	65.25	64.37
Ours ($\tau = 0.75$)	81.35	78.26	76.20
Ours ($\tau = 0.85$)	81.89	80.85	77.79
Ours ($\tau = 0.95$)	82.33	82.32	78.35

F.2 Ablation Study on the Auxiliary Branch

To evaluate the impact of the auxiliary branch, we integrate it into both FreeMatch [8] and SimPro [13] and analyze their performance variations. As demonstrated in Figs. 6 and 7, our analysis reveals that the auxiliary branch exhibits divergent effects across methods. FreeMatch \ddagger (FreeMatch with the auxiliary branch, Fig. 6(a)) selectively improves pseudo-label quality and quantity for both majority classes (e.g., classes 8 and 9) and minority classes (e.g., class 7), unlike the baseline (FreeMatch without the auxiliary branch, Fig. 1(a)). In contrast, SimPro suffers consistent degradation in pseudo-label quality and quantity across nearly all classes when integrated with the auxiliary branch. These trends are further supported by the error rate and utilization rate comparisons in Figs. 3 and 7, which indicate similar performance variations.

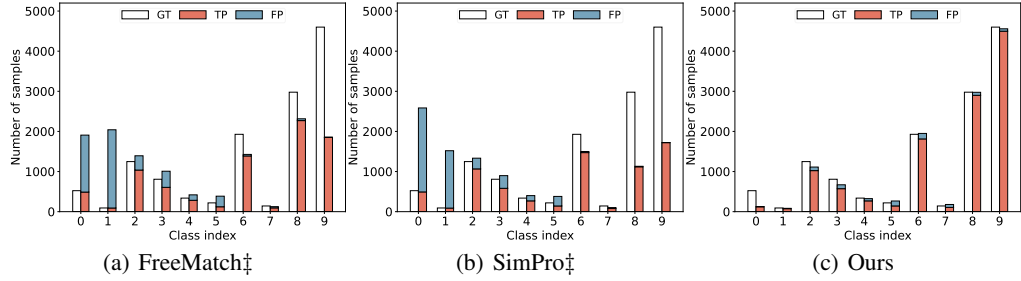


Figure 6: Comparison of pseudo-label predictions among FreeMatch \ddagger [8], SimPro \ddagger [13], and our CPG under arbitrary unlabeled data distribution. GT denotes the ground-truth unlabeled data distribution. TP (FP) denotes the predicted true (false) positive pseudo-labels. The dataset is CIFAR-10-LT with ($N_{max}, M_{max}, \gamma_l, \gamma_u$) = (400, 4600, 50, 50). Our CPG can generate more reliable pseudo-labels than FreeMatch \ddagger and SimPro \ddagger in both minority classes like class 1, 2 and majority classes like class 6, 8, 9. \ddagger indicates that we reproduce baseline methods with the auxiliary branch, similar to our CPG.

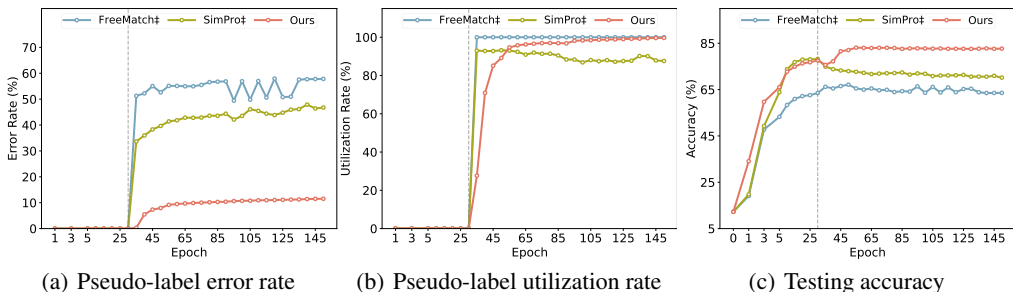


Figure 7: Comparison of pseudo-label error rate (a), pseudo-label utilization rate (b), and testing accuracy (c) among FreeMatch \ddagger [8], SimPro \ddagger [13], and our CPG under arbitrary unlabeled data distribution. The dataset is CIFAR-10-LT with ($N_{max}, M_{max}, \gamma_l, \gamma_u$) = (400, 4600, 50, 50). The vertical gray dotted line indicates the initiation of pseudo-labeling. Our CPG can generate pseudo-labels with a lower error rate and comparable utilization rate, achieving superior testing accuracy compared to both FreeMatch \ddagger and SimPro \ddagger . \ddagger indicates that we reproduce baseline methods with the auxiliary branch, similar to our CPG.

F.3 Ablation Study on the Anchor Distributions

In the main paper, we compare our CPG with ACR† (without anchor distributions) since anchor distributions are typically unknown in real-world scenarios. Here, we further supplement this analysis by comparing CPG with ACR (with anchor distributions) under the assumption that anchor distributions are known. As shown in Tables 14, 15, and 16, our method outperforms ACR even when anchor distributions are known, while ACR relies on this prior knowledge. This demonstrates the robustness and practical applicability of our method.

Table 14: Comparison of accuracy (%) on CIFAR-10-LT ($N_{max} = 400$, $M_{max} = 4600$) with class imbalance ratio $\gamma \in \{100, 150, 200\}$ under different unlabeled data distributions.

Method	$\gamma = 100$			$\gamma = 150$			$\gamma = 200$			Avg.
	Arbitrary	Inverse	Consistent	Arbitrary	Inverse	Consistent	Arbitrary	Inverse	Consistent	
ACR† [14]	60.60 \pm 4.21	62.54 \pm 4.04	73.20 \pm 1.80	48.22 \pm 8.07	51.08 \pm 1.03	68.31 \pm 0.35	50.13 \pm 7.50	53.40 \pm 3.49	65.12 \pm 1.05	59.18 \pm 3.51
ACR [14]	76.18 \pm 0.91	75.72 \pm 1.05	73.27 \pm 0.96	66.69 \pm 2.03	66.68 \pm 1.82	69.34 \pm 3.05	68.91 \pm 3.50	67.25 \pm 1.57	66.48 \pm 4.79	70.06 \pm 2.19
Ours	82.10 \pm 0.74	82.37 \pm 0.15	76.93 \pm 2.68	76.38 \pm 3.87	78.19 \pm 1.63	70.75 \pm 2.13	75.18 \pm 3.28	77.45 \pm 1.44	68.33 \pm 3.94	76.41 \pm 2.21

Table 15: Comparison of accuracy (%) on CIFAR-100-LT ($N_{max} = 50$, $M_{max} = 450$) with class imbalance ratio $\gamma \in \{10, 15, 20\}$ under different unlabeled data distributions.

Method	$\gamma = 10$			$\gamma = 15$			$\gamma = 20$			Avg.
	Arbitrary	Inverse	Consistent	Arbitrary	Inverse	Consistent	Arbitrary	Inverse	Consistent	
ACR† [14]	44.10 \pm 1.59	48.50 \pm 0.86	41.33 \pm 0.41	35.12 \pm 1.36	39.01 \pm 0.38	32.73 \pm 1.74	29.08 \pm 1.11	32.78 \pm 1.59	29.69 \pm 2.94	36.93 \pm 1.33
ACR [14]	50.92 \pm 0.96	50.29 \pm 0.71	50.57 \pm 0.98	44.02 \pm 0.63	43.49 \pm 0.54	44.68 \pm 0.90	41.93 \pm 1.64	39.62 \pm 1.53	42.28 \pm 1.29	45.31 \pm 1.02
Ours	51.48 \pm 0.32	51.46 \pm 0.22	51.22 \pm 0.71	46.26 \pm 1.40	47.88 \pm 0.24	45.94 \pm 1.02	44.17 \pm 1.30	44.17 \pm 1.01	42.66 \pm 0.56	47.25 \pm 0.75

Table 16: Comparison of accuracy (%) on Food-101-LT ($N_{max} = 50$, $M_{max} = 450$) with class imbalance ratio $\gamma \in \{10, 15\}$ and SVHN-LT ($N_{max} = 400$, $M_{max} = 4600$, $\gamma = 100$) under different unlabeled data distributions.

Method	Food-101-LT						SVHN-LT			Avg.	
	$\gamma = 10$			$\gamma = 15$			$\gamma = 100$				
	Arbitrary	Inverse	Consistent	Arbitrary	Inverse	Consistent	Arbitrary	Inverse	Consistent		
ACR† [14]	18.41 \pm 0.75	19.27 \pm 1.12	17.30 \pm 0.58	15.44 \pm 0.50	17.07 \pm 0.61	13.88 \pm 0.73	16.90 \pm 0.72	87.67 \pm 4.60	84.20 \pm 1.58	92.64 \pm 0.50	88.17 \pm 2.23
ACR [14]	21.87 \pm 1.24	22.33 \pm 0.10	21.81 \pm 0.47	19.11 \pm 1.49	19.04 \pm 0.56	18.84 \pm 0.13	20.50 \pm 0.67	88.04 \pm 1.70	90.04 \pm 0.58	89.59 \pm 1.54	89.22 \pm 1.28
Ours	25.98 \pm 0.66	25.52 \pm 0.43	25.24 \pm 0.30	21.88 \pm 0.85	21.27 \pm 0.51	22.11 \pm 0.72	23.67 \pm 0.58	93.99 \pm 0.34	94.74 \pm 0.49	93.45 \pm 0.52	94.06 \pm 0.45

G Relation to Existing Methods

Here, we summarize the difference between our CPG and existing methods (i.e., FixMatch [7], FlexMatch [29], UPS [48], CADR [49], FlexDA [50], DASO [51]).

While CPG adopts confidence-based filtering similar to FixMatch [7] and FlexMatch [29], its key innovation is the controllable self-reinforcing optimization cycle, which incorporates reliable pseudo-labels from the unlabeled dataset into the labeled dataset rather than employing consistency regularization, distinguishing it from existing methods. This cycle operates in three steps: (i) expanding the labeled dataset with reliable pseudo-labels, (ii) constructing a Bayes-optimal classifier, and (iii) iteratively improving pseudo-label quality, forming a theoretically grounded feedback loop. Additionally, CPG ensures full sample utilization via an auxiliary branch and reduces label noise accumulation through a voting-based stabilization technique, which enforces consistent pseudo-label assignments across training steps. As evidenced by the ablation studies in Table 5, these components individually contribute significant performance improvements, with the auxiliary branch and optimization cycle yielding average gains of 1.82 pp and 6.97 pp, respectively.

The goals of UPS [48] and CADR [49] differ from ours. UPS targets poor model calibration in SSL without distribution mismatch and CADR addresses distribution mismatch due to label missing not at random, while our work focuses on handling the unknown and arbitrary unlabeled data distribution. Specifically, UPS mitigates high-confidence incorrect pseudo-labels caused by poor model calibration through uncertainty estimation techniques like MC-Dropout [52], and CADR focuses on resolving classifier bias due to label missing not at random by employing class-aware propensity estimation and dynamic threshold adjustment for pseudo-label selection. Unlike these existing techniques that rely on uncertainty estimation or threshold adjustment, we propose a novel controllable self-reinforcing optimization cycle that operates without distribution estimation or correction, introducing distinct conceptual and methodological innovations. More importantly, our framework is specifically designed to address real-world scenarios with unknown and arbitrary unlabeled data distributions.

While FlexDA [50] relies on estimating the unlabeled data distribution for distribution alignment and pseudo-label generation, our core contribution introduces a controllable self-reinforcing optimization cycle that entirely bypasses unlabeled data distribution estimation. This approach is fundamentally different from FlexDA’s dynamic distribution alignment. Specifically, we iteratively expand the labeled dataset with reliable pseudo-labels, train a Bayes-optimal classifier via logit adjustment on the updated labeled dataset without using the pseudo-label distribution. More importantly, we further theoretically prove that this optimization cycle can significantly reduce the generalization error, whereas FlexDA lacks such theoretical guarantees. Moreover, our auxiliary branch leverages all available samples (without a confidence threshold) to enhance feature learning while preventing the primary branch classifier from error pseudo-labels. Notably, prior methods (e.g., FlexDA [50], SimPro [50], UPS [48], DASO [51]) lack class-aware enhancements for tail classes.

H Limitations

(i) Our CPG assumes that the labeled data is free from noise during training. Consequently, CPG may encounter challenges when adapting to scenarios involving noisy labels. (ii) Our CPG operates under the assumption that labeled data follows a long-tailed distribution, with even tail classes retaining minimal supervision. However, its performance may degrade when labeled data follows a uniform distribution but suffers from extremely limited supervision. Future work will explore extensions to address these limitations and improve model generalization.

I Compute Resources

- CPU: AMD EPYC 7642 48-Core Processor $\times 2$
- GPU: NVIDIA GeForce RTX 4090 24G $\times 1$
- MEM: 500G
- Maximum total computing time: training + testing $\approx 17h$

J Broader Impacts

This paper presents work whose goal is to advance the field of Machine Learning. Specifically, we propose a new realistic long-tailed semi-supervised learning algorithm to improve performance in unknown arbitrary distribution scenarios by expanding the labeled dataset with the progressively identified reliable pseudo-labels from the unlabeled dataset and training the model on the updated labeled dataset with a known distribution, making it unaffected by the unlabeled data distribution. We further theoretically prove that this iterative process can significantly reduce the generalization error under some conditions. There are many potential societal consequences of our work, none of which we feel must be specifically highlighted here.